Thermoelectric Properties of Solution-Processed n-Doped Ladder-Type Conducting Polymers

Wang, Suhao; Sun, Hengda; Ail, Ujwala; Vagin, Mikhail; Persson, Per O. Å.; Andreasen, Jens Wenzel; Thiel, Walter; Berggren, Magnus; Crispin, Xavier; Fazzi, Daniele; Fabiano, Simone

Published in:
Advanced Materials

Link to article, DOI:
10.1002/adma.201603731

Publication date:
2016

Document Version
Peer reviewed version

Thermoelectric Properties of Solution-Processed n-Doped Ladder-Type Conducting Polymers

Suhao Wang, Hengda Sun, Ujwala Ail, Mikhail Vagin, Per O. Å. Persson, Jens W. Andreasen, Walter Thiel, Magnus Berggren, Xavier Crispin, Daniele Fazzi and Simone Fabiano

Journal Article

Original Publication:

Suhao Wang, Hengda Sun, Ujwala Ail, Mikhail Vagin, Per O. Å. Persson, Jens W. Andreasen, Walter Thiel, Magnus Berggren, Xavier Crispin, Daniele Fazzi and Simone Fabiano, Thermoelectric Properties of Solution-Processed n-Doped Ladder-Type Conducting Polymers, Advanced Materials, 2016.
http://dx.doi.org/10.1002/adma.201603731

DOI: 10.1002/((please add manuscript number))
Article type: Communication

Thermoelectric properties of solution-processed n-doped ladder-type conducting polymers

Suhao Wang, Hengda Sun, Ujwala Ail, Mikhail Vagin, Per O. Å. Persson, Jens W. Andreasen, Walter Thiel, Magnus Berggren, Xavier Crispin, Daniele Fazzi, Simone Fabiano**

Dr. S. Wang, Dr. H. Sun, Dr. U. Ail, Dr. M. Vagin, Prof. M. Berggren, Prof. X. Crispin, Dr. S. Fabiano
Laboratory of Organic Electronics, Department of Science and Technology, Linköping University, SE-60174, Norrköping, Sweden.
E-mail: simone.fabiano@liu.se

Prof. Per O. Å. Persson
Thin Film Physics Division, Department of Physics Chemistry and Biology, Linköping University, SE-581 83 Linköping, Sweden.

Dr. J. W. Andreasen
Technical University of Denmark, Department of Energy Conversion and Storage, Frederiksborgvej 399, 4000 Roskilde, Denmark.

Prof. W. Thiel, Dr. D. Fazzi
Max-Planck-Institut für Kohlenforschung, Kaiser-Wilhelm-Platz 1, D-45470 Mülheim an der Ruhr, Germany.
E-mail: fazzi@mpi-muelheim.mpg.de

Keywords: conducting polymers, n-doping, polarons, ladder-type, broken symmetry DFT.

Conjugated polymers are an emerging class of materials for large-area solid-state energy conversion and storage applications.[1] These materials enable new paths towards a more sustainable energy landscape without the need of expensive, or even toxic, metal-based compounds. The possibility to harness heat wasted in our daily life by converting a temperature gradient into electricity via thermoelectric generators (TEGs) is attractive, when compared to the organic Rankine cycle, despite their low efficiency. Indeed, TEG is an electronic device without

mechanical parts that wear out and it can be easily scaled down for various applications such as powering sensors.[2] Recently, conducting polymers have been identified as potential thermoelectric materials for the low temperature range (< 200 °C).[3] Their constituting atomic elements (e.g. C, N, O, S) are from millions to billions of times more abundant than those present in state-of-the-art thermoelectric materials for low temperature applications, for instance BiTeSb alloys. Moreover, polymers are lightweight and allow for mechanically flexible devices. Driven by their versatile chemical synthesis, conducting polymers can be scaled up for mass production of thermoelectric devices at relatively low cost, via room-temperature and solution-based manufacturing processes.[4] However, building efficient thermoelectric devices requires high-performance complementary *p*-type (hole-transporting) and *n*-type (electron-transporting) materials. Up to date, all-organic thermoelectric devices have been difficult to manufacture due to the limitations encountered by the *n*-type organic semiconductors. Unlike their *p*-type counterparts, displaying conductivity up to 1000 S cm^{-1},[5] *n*-doped conducting polymers typically suffer from a low electron conductivity (σ), primarily due to their low electron affinity that strongly restricts the *n*-doping level. In thermoelectric applications, low σ translates into low power factor (defined as $S^2\sigma$, with S being the Seebeck coefficient) and ultimately into a low thermoelectric figure of merit ($ZT = S^2\sigma/kT$, with k the thermal conductivity and T the temperature). Like for other conductors, heat is transported by phonons and charge carriers in conducting polymers;[6] yet, their unique feature is an intrinsically low phonon contribution, which leads to low k values (0.3-0.8 W m^{-1} K^{-1}). The other two parameters defining ZT, i.e. σ and S, are interrelated as a function of the charge carrier concentration of the material, typically featuring opposite trends which lead to a maximum value of $S^2\sigma$ for a certain doping level.[7] The optimization of σ and S, together with a proper understanding of the charge (i.e. polaron)

transport mechanisms, represents the key point in maximizing the thermoelectric properties of conducting polymers. Today, the record values of *ZT* for *p*-type conducting polymers are 0.25,[3] 0.31[8] and 0.42[9] at room temperature.

The best performing *n*-type organic thermoelectric materials up to date are organometallic polymers, featuring an electrical conductivity as high as 40 S cm^{-1} and a power factor of up to 66 μW m^{-1} K^{-2}.[10] However, these materials are not directly processable from solution, thus severely restricting their extensive application. With the exception of just a few polymers based on benzodifurandione-phenylenevinylene derivatives, showing *n*-type conductivity as high as 14 S cm^{-1},[11] solution-processed *n*-doped conducting polymers show typically conductivities of less than 10^{-2} S cm^{-1}. Recently, Chabinyc et al. reported a maximum conductivity of ~10^{-3} S cm^{-1} for donor-acceptor polymers, such as poly{[*N*,*N*′-bis(2- octyldodecyl)-naphthalene-1,4,5,8-bis(dicarboximide)-2,6-diyl]-*alt*-5,5′-(2,2′-bithiophene)} [P(NDI2OD-T2)] doped with benzimidazol-based dopants (e.g., DMBI).[12] It is suspected that a poor solubility of the dopant in this polymer matrix results in a low doping level, thus causing the low σ. However, similar σ values have been reported for P(NDI2OD-T2) doped with dimer dopants that react effectively and quantitatively by electron transfer,[13] which instead indicates an intrinsic upper limit for the electron conductivity of this class of materials. Theoretical and experimental studies on donor-acceptor polymers reveal that, despite the high carrier mobility, polarons are localized on the chains.[14] This results in a charge transport that mainly occurs along the polymer backbone and is macroscopically supported by short-range inter-molecular aggregation.[15] Recent measurements on novel donor-acceptor perylenediimide- and naphthalenediimide-based polymers suggest a correlation between the delocalization of polarons and the macroscopic

conductivity.[16] However, the relationship between chemical structure, polaron localization/delocalization and doping efficiency remains unclear.

Here we show that ladder-type conducting polymers, such as solution-processable *n*-type polybenzimidazobenzophenanthroline (BBL),[17] can achieve *n*-type conductivities as high as 2.4 S cm^{-1} when doped with strong reducing agents such as tetrakis(dimethylamino)ethylene (TDAE). These remarkable values are three orders of magnitude higher than those measured for P(NDI2OD-T2), here used as the reference model system. Insights into the polaronic properties of both polymers were gained through Density Functional Theory (DFT) calculations. An adequate description of polarons in long BBL oligomers (approaching the polymer limit) requires the use of the unrestricted DFT broken symmetry (UDFT-BS) approach. This aspect, of importance by itself, reflects the stability of polarons in extended π-conjugated systems and suggests that the polaron wavefunction in narrow-band-gap π-conjugated ladder-type polymers is of multiconfigurational character. The computed polaron delocalization length for the linear - '*torsion-free*' - homo-polymer BBL is larger than that of the *distorted* donor-acceptor polymer P(NDI2OD-T2). According to recent findings by Bao et al.,[16] this might suggest a higher intra-chain polaron mobility for BBL than P(NDI2OD-T2). In this frame, the observed high BBL electron conductivity can be already rationalized at the single-chain scale. By carefully modulating the doping levels, we optimized the Seebeck coefficient and power factor, reaching values of ~0.43 μW m^{-1} K^{-2}, which are one order of magnitude higher than those achieved in P(NDI2OD-T2).

Scheme 1 illustrates the chemical structures of BBL, P(NDI2OD-T2) and TDAE. Both BBL and P(NDIOD-T2) have several compelling properties including good solution processability, air stability, and high field-effect mobilities.[17-18] However, unlike P(NDI2OD-T2), BBL is not a

donor-acceptor polymer and, most notably, it shows a highly rigid and planar polymer backbone, which leads to unusual high glass transition temperature (>500 °C) and high thermal stability.[17] TDAE was chosen as the *n*-dopant since it has successfully been used for the optimization of the thermoelectric figure of merit of *p*-type conducting polymers such as poly(3,4-ethylenedioxythiophene) (PEDOT).[3, 19] It is then appealing to explore this material in the fabrication of printed thermoelectric generators, as it allows for the simultaneous optimization of oxidation levels in both *p*- and *n*-doped polymers.

To analyze the changes associated with the doping level of the *n*-type polymers exposed to TDAE vapors, UV-Vis-NIR spectroscopy was performed on thin films for different exposure times. **Figure 1**a shows optical absorption spectra of BBL films before and after TDAE exposure. An intense absorption peak (A) at around 580 nm is clearly evident for the pristine film, similarly to what has previously been reported for pristine (undoped) BBL films.[20] Based on our TD(DFT) calculations performed on BBL oligomers featuring different repeat units (BBL_n, n = 1, 2, 4, 8, see Supporting Information), band A is associated with the S_0–S_1 transition, with S_1 being a Frenkel-like exciton delocalized over up to six repeat units. After TDAE treatment, a clear reduction of band A is observed together with the appearance of a new broad band (B) at about 900 nm. TD(UDFT-BS) calculations performed on the longer oligomer (BBL_8, *vide* Figure 1c and Supporting Information) well reproduce the intensity reduction and broadness of band A, and the appearance of the new band B, ascribed to polaron-induced transitions. Although DFT calculations on oligomer models tend to overestimate the transitions energies,[21] the computed spectral shape and band intensity ratio are consistent with the experimental trends; furthermore, our assignments are also corroborated by previous reports on

electrochemically-doped BBL thin films,[20] thus confirming the successful doping of the polymer.

Figure 1b reports the UV-Vis-NIR spectra of pristine and TDAE-doped P(NDI2OD-T2) thin films. In the undoped pristine state, P(NDI2OD-T2) shows the typical absorption features already reported in literature,[22] which are assigned to a high-energy π–π* transition (D') at 390 nm and a broad, low-energy band (A') centered at 705 nm, mainly associated to an intramolecular charge transfer between the NDI and the bithiophene units. This structured low-energy absorption feature represents also a clear spectroscopic fingerprint of aggregated species. *n*-doping is accompanied by a quenching of band A', along with the rising of two absorption bands (C' and B') at roughly 500 and 820 nm, respectively. In addition, band D' shifts towards longer wavelengths (Figure 1b) as the *n*-doping level increases. From TD(UDFT) calculations conducted on long charged P(NDI2OD-T2) oligomers (n = 4, 5), we can assign the absorption bands of doped films to polaronic species (see Figure 1b and details in Supporting Information). Our measured spectra and computational assignments are also consistent with the formation of radical anion species, as found by *in situ* spectroelectrochemistry[23] and charge modulation spectroscopy measurements,[24] assuring the successful doping of P(NDI2OD-T2).

The electrical properties of BBL films were investigated before and after exposure to TDAE vapors in an inert environment. **Figure 2**a shows the electrical conductivity (σ) of *n*-doped BBL film as a function of the exposure time (i.e. *n*-doping time). Before exposure, BBL is in its undoped pristine state and shows an electrical conductivity as low as ca. 1×10^{-7} S cm^{-1}. After exposure to TDAE vapors (3 h, at room temperature), the electrical conductivity dramatically increases, reaching a value as high as 1.7 ± 0.6 S cm^{-1}, almost seven orders of magnitude higher than that of the pristine state. These values approach those reported for electrochemically-doped

BBL films (about 2 S cm^{-1}),[20] indicating a strong chemical doping ability of TDAE. Interestingly, no changes in the final electrical conductivity are observed for longer exposure times (> 20h) and even after several weeks of storage in nitrogen. The large increase in the electrical conductivity is in agreement with the rise of polaron absorption bands in the UV-Vis-NIR spectra, corroborating the successful *n*-doping of BBL films. Compared to chemically *n*-doped P(NDI2OD-T2), BBL shows an electrical conductivity up to three orders of magnitude larger (see Figure 2a). Upon *n*-doping, P(NDI2OD-T2) conductivity reaches a maximum of 5×10^{-3} S cm^{-1}, which then monotonically decreases for longer exposure time. The observed maximum conductivity value and trend for P(NDI2OD-T2) are comparable to previous reports,[12-13, 16] assuring that films here investigated are representative of a high-performance material. Note that the oxidation potential of TDAE (ca. –1 V vs. Fc/Fc^{+})[25] is comparable to the reduction potential of the BBL and P(NDI2OD-T2) (see Figure S1, Supporting Information). Thus, the doping more likely takes place through electron transfer from the dopant to the semiconducting polymer. As both BBL and P(NDI2OD-T2) show equal electron affinities (EA = –4.0 eV),[26] we exclude that the difference in the electrical conductivity of the two polymers, upon doping, is due to different energy-level values.

The maximum electrical conductivity of doped BBL and P(NDI2OD-T2), normalized to 300 K, is plotted in Figure 2b as function of the inverse temperature from 200 to 300 K. The temperature dependence of conductivities is in agreement with a quasi-1D hopping transport (see Figure S2). At high temperatures, the transport is through nearest neighbor hopping and the corresponding Arrhenius activation energies (E_A) are found to be 0.28 eV and 0.12 eV for P(NDI2OD-T2) and BBL, respectively. The former is comparable to prior results of P(NDI2OD-T2) doped with

DMBI[12] or $[RhCp_2]_2$,[27] and is in agreement with theoretically predicted values derived in the polymer limit.[14]

The difference in the electrical conductivity between BBL and P(NDI2OD-T2) can be ascribed to their intrinsic (i.e. molecular) structural and polaronic properties. We then compared the optimized UDFT structures for the longest charged oligomers (i.e. anions) considered in this study, namely BBL_8 and $P(NDI2OD\text{-}T2)_5$ (Supporting Information). In the charged state, BBL has a flat-planar structure, maintaining the intra-molecular order over a long range. P(NDI2OD-T2) shows, instead, a distorted chain, with pronounced dihedral angles (~50°-70°) between the single conjugated units. These structural differences may have an effect on the polaron delocalization length and the activation energy for charge transport, leading to a low E_A for the structural ordered BBL polaron, whereas high E_A should arise for the more structurally disordered P(NDI2OD-T2).

In the case of BBL oligomers, when the chain length and hence the π-electron delocalization increases (approaching the polymer limit), the unrestricted DFT solution (UDFT) becomes unstable and is thus not capable of describing the polaronic state in a proper manner. For this purpose, the broken symmetry formalism (UDFT-BS) is better suited. More specifically (see details in Supporting Information), while short BBL oligomers (n = 1,2) do not show any DFT *instability* in the charged state, longer chains (n = 4, 8) do. The corresponding stabilization energy ($\Delta E = E(UDFT\text{-}BS) - E(UDFT)$) is -0.27 eV for BBL_4 and -0.42 eV for BBL_8, respectively. This implies that for long oligomers (here n = 4 and 8), representative of the polymer chains, the UDFT-BS approach should be adopted to describe the polaronic properties, in the DFT framework. A detailed comparison between UDFT *vs.* UDFT-BS results (i.e. electronic transition energies, polaron structural relaxations, etc.) is reported in the Supporting

Information. For the case of P(NDI2OD-T2), instead, no instability in the electronic structure of the charged state is encountered when increasing the oligomer length, confirming that UDFT is an adequate approach for the description of the polaronic properties for such donor-acceptor systems.

In analogy to biradicaloid systems,[28] the instability occurring at the UDFT level for long BBL oligomers can be traced back to the *symmetry-dilemma* or symmetry-breaking problems.[29] It is related to a multiconfigurational character of the ground state wavefunction. In the case of BBL, a fully satisfactory description of the polaron electronic structure would thus require the use of multiconfigurational wavefunction methods or hybrid approaches (e.g. multiconfigurational pair-density functional theory),[30] which are however still impractical for such large systems with current state-of-the art computational resources.

In **Figure 3** we compare the spin (i.e. α and β) density distributions of the longest BBL (n = 8) and P(NDI2OD-T2) (n = 5) oligomers here investigated. The polaron is more delocalized in BBL (UDFT-BS) than in P(NDI2OD-T2) (UDFT): the spin density and the structural relaxations (for the latter see Supporting Information) extend over almost three repeating units in BBL, rather than only one in P(NDI2OD-T2). We believe that this is related to the planar molecular structure of BBL, which allows for more *homogenous* structural relaxations induced by the extra electron. In fact, just considering the single repeat polymer unit (n = 1) the polaron is fully delocalized in BBL, while in P(NDI2OD-T2) it is mostly localized on the NDI2OD moiety due to the D-A character of the building blocks, thus causing asymmetric relaxations along the chain.[14, 31]

Grazing-incidence wide-angle X-ray scattering (GIWAXS) and transmission electron microscopy (TEM) were performed to investigate the crystalline morphology and the effect of doping on the polymer crystal structures. The TEM image of undoped P(NDI2OD-T2) films

reveals a fiber-like structure qualitatively similar to previously published observations in the neat polymer films.[32] The GIWAXS is also fully consistent with the known diffraction pattern of P(NDI2OD-T2) and shows a preferential face-on orientation (Figure S3).[15] After doping, the fiber-like structure in the TEM image is less visible while from the GIWAXS the in-plane (100) and (200) lamellar reflections decrease in intensity, such that only the first-order (100) and (001) reflections are visible. In the out-of-plane direction, the (010) peak corresponding to the π-π stacking is smoothed by doping (see Figure S4). The diffraction pattern of TDAE-doped P(NDI2OD-T2) is qualitatively similar to that recently reported for the same polymer doped with dimer dopants.[16] In the case of BBL, the GIWAXS data are in good agreement with previously measured diffraction pattern of undoped films.[33] Upon doping, the texture is not affected, whereas the polymer structure is substantially changed, as evidenced by a rather large shift of the strong (100) lamellar peak, and the concomitant occurrence of an intermediate peak at a lower scattering angle (see Figures S4). This could be interpreted as a doubling of the unit cell in the direction of the lamellar packing, indicating a change in structure caused by doping. Overall, for both pristine and doped polymers, we observe that BBL exhibits the most pronounced π-stacking, which indicates very high ordering of this polymer.

The Seebeck coefficient of BBL and P(NDI2OD-T2) thin films were also measured as a function of the TDAE exposure time. To minimize the error in determining *S*, we used an electrode configuration which takes into account the effect of the contact geometry.[34] The Seebeck coefficient of BBL decreases by a factor of 7 upon exposing the polymer to the TDAE vapors (**Figure 4**a). *S* is initially about –400 ± 25 μV K^{-1} for a σ of around 3×10^{-4} S cm^{-1}, then reaching its minimum of –60± 4 μV K^{-1} for σ = 1 S cm^{-1}. Notably, the sign of the thermovoltage is consistent with electrons being the majority carrier (Figure S5, Supporting

Information). In comparison, the Seebeck coefficient of P(NDI2OD-T2) decreases from −790 ± 14 μV K^{-1} to −150 ± 5 μV K^{-1} when σ increases from 1 × 10^{-4} S cm^{-1} to about 3 × 10^{-3} S cm^{-1} (Figure 4b). For long exposure times, σ reduces as observed before, and thus the extraction of S is not straightforward, as the resistance of P(NDI2OD-T2) changes dramatically while heating the substrate (Figure S6, Supporting Information). Note that similar S values are obtained regardless of the film thickness and when DMBI is used as dopant agent. Since σ increases while S decreases, at higher doping levels, the power factor ($S^2\sigma$) reaches an optimum at a specific exposure time (doping level). Note that since the electronic contribution to the thermal conductivity is expected to be almost negligible for the range of electrical conductivity in our samples, we only focus our study on the optimization of the power factor. For BBL, a maximum $S^2\sigma$ of 0.43 μW m^{-1} K^{-2} is obtained, which is one order of magnitude higher than that of P(NDI2OD-T2) (0.013 μW m^{-1} K^{-2}). Note that the latter is one order of magnitude lower than previously reported for P(NDI2OD-T2), which could be due to contact geometry effect.[34]

We have attempted to interpret the magnitude of the Seebeck coefficients consistently in terms of variable-range hopping disorder (VRH) model.[35] Similar analysis has been used to explain comparable measurements in amorphous silicon[36] and polymers.[37] The Seebeck coefficient

$$S = \frac{\int (E - E_F)\sigma(E)dE}{eT \int \sigma(E)dE} \quad (1)$$

is determined by the difference between the Fermi energy level (E_F) and the transport energy level (E). In Eq. (1), $\sigma(E)$ is the conductivity distribution function, T the temperature, and e the charge of the carrier. In the frame of the variable-range hopping model, where the transport is

assumed to be dominated by a characteristic hop from the equilibrium energy to a relatively narrow transport energy E^* (see inset Figure 4c), Eq. (1) becomes

$$S = \frac{(E^* - E_F)}{eT} \quad (2)$$

In the hopping regime, E_F shifts towards the transport energy E^* by increasing the charge carrier density (i.e. the doping level). This explains the typical trend of *S* of decreasing upon increasing the doping level [i.e. exposure time (see Figure 4a)]. The Seebeck coefficient of P(NDI2OD-T2) is higher than BBL, possibly due to a difference in doping level and/or a difference in extension of the charge carrier as shown in the VRH model.[38] The potentially lower doping level of P(NDI2OD-T2) compared to BBL is not due to the EA, which is the same for both polymers, but rather to the D–A character of P(NDI2OD-T2), which may cause inefficient doping.[39]

A second effect rarely discussed but recently pinpointed in a theoretical study[38] is that the evolution of *S* with doping level is very dependent on the degree of localization of the carriers. If the localization length is small, S varies quickly with doping level. If the carrier is extended instead, then S varies slowly with doping level.[38] This means that for equal doping level, and equal Gaussian width, the extension of the localized state describing the carrier is affecting the Seebeck coefficient. BBL has a larger polaron extension compared to P(NDI2OD-T2), and this could be one origin of the low *S* reported in Figure 4a. Note that the weak temperature dependence of *S*, compared with that of σ (Figure 2b), supports our choice of using a VRH model to interpret qualitatively our results. Considering a VRH (with percolation) model for charge transport, using a Gaussian density of states, the slope of *S* versus *T* is related to the degree of disorder.[40] When BBL and P(NDI2OD-T2) are doped to the maximum conductivity,

BBL shows a weaker temperature dependence of S ($\partial S/\partial(1/T)$ = 0.05 eV) than P(NDI2OD-T2) (0.13 eV) (see Figure S7). This may suggest a lower disorder in BBL compared to P(NDI2OD-T2), as indicated by the GIWAXS data.

As a direct measurement of the carrier concentration in organic materials is difficult, due to their low mobility and energetic disorder, it is simplest to discuss the variation of S as a function of σ, as shown in Figure 4b. BBL follows the empirical relation of $S \propto \sigma^{-1/4}$, as already observed for other semiconducting polymers,[41] while P(NDI2OD-T2) shows a stronger dependence ($S \propto \sigma^{-1/2}$). Although the origin of this empirical trend is not clearly understood yet, the different slope could be due to differences in the molecular order, as observed for stretched polyaniline[42], or to a different polaron extension, in agreement with the DFT results.

In conclusion, we demonstrated that linear – '*torsion-free*' – ladder-type conducting polymers, such as BBL, can reach conductivity values that are three orders of magnitude higher than those of *distorted* donor-acceptor polymer [e.g. P(NDI2OD-T2)]. This is an important and general material design rule for optimizing the thermoelectric properties of conducting polymers. A realistic DFT description of polarons in long BBL oligomers (approaching the polymer limit) is provided by the broken symmetry approach. The computed polaron and spin delocalization lengths are larger in BBL than in P(NDI2OD-T2), suggesting an easier intra-molecular transfer, thus a higher polaron mobility along the chain for the ladder-type polymer. In this frame, the high electron conductivity of BBL can be already rationalized at the single-chain level. The optimized thermoelectric power factor of BBL reaches values that are one order of magnitude higher than those observed for P(NDI2OD-T2). These results provide a simple picture that clarifies the relationship between the backbone structure of the polymer and the polaron

delocalization length, setting molecular-design guidelines for next-generation conjugated polymers.

Experimental Section

Film preparation and doping: All devices were fabricated using glass substrates cleaned sequentially in acetone, water and isopropanol, followed by drying step with nitrogen. P(NDI2OD-T2) (M_n = 29.5 KDa and PDI = 2.1, Polyera ActivInk N2200, purchased from Polyera Corp.) was dissolved in o-dichlorobenzene at the concentration of 5 mg/mL, and the solution was stirred at 70 °C for ca.1 hour to allow complete dissolution of the polymer. After stirring, the solution was spin-coated onto the glass substrates at 1000 rpm for 40s. Prior to doping, the films were thermally annealed at 110 °C under nitrogen atmosphere for 10min, and cooled down naturally to room temperature. BBL (purchased from Sigma-Aldrich, intrinsic viscosity [η]=0.58 dL g^{-1} in concentrated sulfuric acid at 25 °C[43]) was dissolved in methanesulfonic acid (MSA) at the concentration of 5 mg/mL. The solution was stirred at 70 °C for ca.1 hour to allow complete dissolution of the polymer. After stirring, the solution was spin-coated onto the glass substrates at 600 rpm for 2 min. The BBL films were then dipped immediately after spin coating into deionized water to remove MSA. All the BBL films were dried on a hotplate at 70 °C in glovebox under nitrogen atmosphere overnight after removal from water. Prior to doping, the films were thermally annealed at 110 °C under nitrogen atmosphere for 10 min. The polymer films, deposited on glass substrates, were exposed to the TDAE vapor inside an airtight glass bottle (20 mL in volume filled with 1 mL liquid TDAE), following a procedure reported earlier.[44] The exposure took place inside a nitrogen-filled glovebox and was halted at the required time by removing the polymeric films from the TDAE bottle.

Optical and electrical characterization: Absorption spectra of BBL and P(NDI2OD-T2) films were conducted at room temperature using an UV-vis-NIR spectrophotometer (PerkinElmer Lambda 900). Electrical conductivity and Seebeck coefficient measurements were performed inside a nitrogen-filled glovebox using a semiconductor parameter analyzer (Keithley 4200-SCS). Bottom gate/bottom contacts field-effect mobility were used to extract the electron mobilities of P(NDI2OD-T2) and BBL, that are 1.5×10^{-2} cm^2 $V^{-1}s^{-1}$ and 2.3×10^{-3} cm^2 $V^{-1}s^{-1}$, respectively. For conductivity measurements reported in Fig. 2a-b, 12-nm-thick Au electrodes with a 3-nm-thick Ti adhesion layer (L/W= 30μm/1000μm) were fabricated on glass substrates prior to active layer deposition. For the Seebeck coefficient measurements reported in Fig. 4a for a given doping time at room temperature (thermally evaporated gold electrodes with L/W= 0.5 mm/15 mm), the samples were fixed in between a pair of Peltier modules to maintain the desired temperature difference. Here, ΔT was measured by means of thermocouples. Note that in case of temperature dependent Seebeck coefficient measurements reported in Fig. S7 (photolithograpically defined electrodes with L/W= 30μm/1300μm), an integrated heater positioned parallel to the channel electrode/temperature sensors was used to create the temperature difference. The distance between the heater and the hot sensor is 20 μm. In this case, ΔT was measured using gold thermistors. The width of the heater and the thermistors is 20 μm. The Seebeck coefficient was calculated from the shift in the current-voltage curves caused by the thermal voltage $S\Delta T$.

Computational methods: BBL and P(NDI2OD-T2) were modeled through an oligomer approach via DFT calculations using the ωB97X-D3 functional and the 6-31G* basis set. Neutral and charged (i.e. radical-anion) species were described at the restricted and unrestricted DFT level of theory, respectively. The stability of the DFT solution was tested and verified in all cases via the

spin-unrestricted broken symmetry (BS) approach.[45] No instability was found for the neutral species of both polymers and for the charged species of P(NDI2OD-T2), confirming that the restricted DFT treatment is appropriate for these systems. In the case of the charged species of BBL, an instability was found for oligomers with four or more repeat units, for which the UDFT-BS solution was most stable; the stabilization energy is given by the difference $\Delta E = E(\text{UDFT-BS}) - E(\text{UDFT})$. All structures, namely BBL (n = 1, 2, 4, 8) and P(NDI2OD-T2) (n = 4, 5), were optimized in the neutral and charged states (using their most stable DFT solution). For each oligomer and for each electronic state (neutral and charged), vertical electronic transitions were computed at the TDDFT level (or TDUDFT-BS when appropriate). For the description of the polaron species, an assumption of at most one charge per each oligomer is made due to the low doping level. All calculations were performed using Gaussian09.[46]

Supporting Information
Supporting Information is available from the Wiley Online Library or from the author.

Acknowledgements
SW, HS and UA contributed equally to this work. The authors acknowledge support from the Knut and Alice Wallenberg foundation (project “Tail of the sun”), the Swedish Foundation for Strategic Research (Synergy project). SF gratefully acknowledges funding by the Swedish Governmental Agency for Innovation Systems - VINNOVA (No. 2015-04859) and the Advanced Functional Materials Center at Linköping University (No. 2009-00971). DF kindly acknowledges the Alexander von Humboldt foundation for a postdoctoral fellowship. POÅP acknowledges the Knut and Alice Wallenberg Foundation for support of the electron microscopy laboratory at Linköping University.

Received: ((will be filled in by the editorial staff))
Revised: ((will be filled in by the editorial staff))
Published online: ((will be filled in by the editorial staff))

[1] a) Y. Liang, Z. Chen, Y. Jing, Y. Rong, A. Facchetti, Y. Yao, J. Am. Chem. Soc. 2015, 137, 4956; b) A. Facchetti, Chem. Mater. 2011, 23, 733.
[2] A. P. Joseph, IEEE Pervasive Computing 2005, 4, 18.
[3] O. Bubnova, Z. U. Khan, A. Malti, S. Braun, M. Fahlman, M. Berggren, X. Crispin, Nat. Mater. 2011, 10, 429.
[4] M. Berggren, D. Nilsson, N. D. Robinson, Nat. Mater. 2007, 6, 3.
[5] O. Bubnova, Z. U. Khan, H. Wang, S. Braun, D. R. Evans, M. Fabretto, P. Hojati-Talemi, D. Dagnelund, J.-B. Arlin, Y. H. Geerts, S. Desbief, D. W. Breiby, J. W. Andreasen, R. Lazzaroni, W. M. Chen, I. Zozoulenko, M. Fahlman, P. J. Murphy, M. Berggren, X. Crispin, Nat. Mater. 2014, 13, 190.
[6] a) J. Liu, X. Wang, D. Li, N. E. Coates, R. A. Segalman, D. G. Cahill, Macromolecules 2015, 48, 585; b) A. Weathers, Z. U. Khan, R. Brooke, D. Evans, M. T. Pettes, J. W. Andreasen, X. Crispin, L. Shi, Adv. Mater. 2015, 27, 2101.
[7] a) A. Shakouri, Annual Review of Materials Research 2011, 41, 399; b) G. J. Snyder, E. S. Toberer, Nat Mater 2008, 7, 105.
[8] S. H. Lee, H. Park, S. Kim, W. Son, I. W. Cheong, J. H. Kim, Journal of Materials Chemistry A 2014, 2, 7288.
[9] G. H. Kim, L. Shao, K. Zhang, K. P. Pipe, Nat Mater 2013, 12, 719.
[10] Y. Sun, P. Sheng, C. Di, F. Jiao, W. Xu, D. Qiu, D. Zhu, Adv. Mater. 2012, 24, 932.
[11] K. Shi, F. Zhang, C.-A. Di, T.-W. Yan, Y. Zou, X. Zhou, D. Zhu, J.-Y. Wang, J. Pei, J. Am. Chem. Soc. 2015, 137, 6979.
[12] R. A. Schlitz, F. G. Brunetti, A. M. Glaudell, P. L. Miller, M. A. Brady, C. J. Takacs, C. J. Hawker, M. L. Chabinyc, Adv. Mater. 2014, 26, 2825.
[13] B. D. Naab, S. Zhang, K. Vandewal, A. Salleo, S. Barlow, S. R. Marder, Z. Bao, Adv. Mater. 2014, 26, 4268.
[14] D. Fazzi, M. Caironi, C. Castiglioni, J. Am. Chem. Soc. 2011, 133, 19056.
[15] S. Wang, S. Fabiano, S. Himmelberger, S. Puzinas, X. Crispin, A. Salleo, M. Berggren, Proc. Natl. Acad. Sci. USA 2015, 112, 10599.
[16] B. D. Naab, X. Gu, T. Kurosawa, J. W. F. To, A. Salleo, Z. Bao, Adv. Electron. Mater. 2016, 1600004. doi:10.1002/aelm.201600004.
[17] A. Babel, S. A. Jenekhe, J. Am. Chem. Soc. 2003, 125, 13656.
[18] H. Yan, Z. Chen, Y. Zheng, C. Newman, J. R. Quinn, F. Dötz, M. Kastler, A. Facchetti, Nature 2009, 457, 679.
[19] H. Wang, J.-H. Hsu, S.-I. Yi, S. L. Kim, K. Choi, G. Yang, C. Yu, Adv. Mater. 2015, 27, 6855.
[20] K. Wilbourn, R. W. Murray, Macromolecules 1988, 21, 89.
[21] a) A. l. D. Laurent, D. Jacquemin, Int. J. Quantum Chem 2013, 113, 2019; b) H. Sun, J. Autschbach, Journal of Chemical Theory and Computation 2014, 10, 1035.
[22] M. Schubert, D. Dolfen, J. Frisch, S. Roland, R. Steyrleuthner, B. Stiller, Z. H. Chen, U. Scherf, N. Koch, A. Facchetti, D. Neher, Adv. Energy Mater. 2012, 2, 369.
[23] D. Trefz, A. Ruff, R. Tkachov, M. Wieland, M. Goll, A. Kiriy, S. Ludwigs, J. Phys. Chem. C 2015, 119, 22760.
[24] M. Caironi, M. Bird, D. Fazzi, Z. H. Chen, R. Di Pietro, C. Newman, A. Facchetti, H. Sirringhaus, Adv. Funct. Mater. 2011, 21, 3371.
[25] C. Burkholder, W. R. Dolbier, M. Médebielle, The Journal of Organic Chemistry 1998, 63, 5385.

[26] a) M. M. Alam, S. A. Jenekhe, Chem. Mater. 2004, 16, 4647; b) S. Fabiano, H. Yoshida, Z. Chen, A. Facchetti, M. A. Loi, ACS Appl. Mater. Interfaces 2013, 5, 4417.
[27] Y. B. Qi, S. K. Mohapatra, S. B. Kim, S. Barlow, S. R. Marder, A. Kahn, Appl. Phys. Lett. 2012, 100, 4.
[28] a) D. Fazzi, E. V. Canesi, F. Negri, C. Bertarelli, C. Castiglioni, Chemphyschem 2010, 11, 3685; b) J. Casado, R. Ponce Ortiz, J. T. Lopez Navarrete, Chem. Soc. Rev. 2012, 41, 5672; c) M. Nakano, B. Champagne, Wiley Interdisciplinary Reviews: Computational Molecular Science 2016, 6, 198.
[29] a) J. P. Perdew, A. Savin, K. Burke, Physical Review A 1995, 51, 4531; b) C. D. Sherrill, M. S. Lee, M. Head-Gordon, Chem. Phys. Lett. 1999, 302, 425; c) P.-O. Löwdin, Physical Review 1955, 97, 1474.
[30] G. Li Manni, R. K. Carlson, S. Luo, D. Ma, J. Olsen, D. G. Truhlar, L. Gagliardi, Journal of Chemical Theory and Computation 2014, 10, 3669.
[31] D. Fazzi, M. Caironi, Phys. Chem. Chem. Phys. 2015, 17, 8573.
[32] C. J. Takacs, N. D. Treat, S. Krämer, Z. Chen, A. Facchetti, M. L. Chabinyc, A. J. Heeger, Nano Lett. 2013, 13, 2522.
[33] A. L. Briseno, S. C. B. Mannsfeld, P. J. Shamberger, F. S. Ohuchi, Z. Bao, S. A. Jenekhe, Y. Xia, Chem. Mater. 2008, 20, 4712.
[34] S. v. Reenen, M. Kemerink, Org. Electron. 2014, 15, 2250.
[35] W. C. Germs, K. Guo, R. A. J. Janssen, M. Kemerink, Phys. Rev. Lett. 2012, 109, 016601.
[36] H. Overhof, W. Beyer, Philosophical Magazine Part B 1981, 43, 433.
[37] a) Y. Xuan, X. Liu, S. Desbief, P. Leclère, M. Fahlman, R. Lazzaroni, M. Berggren, J. Cornil, D. Emin, X. Crispin, Physical Review B 2010, 82, 115454; b) D. Venkateshvaran, M. Nikolka, A. Sadhanala, V. Lemaur, M. Zelazny, M. Kepa, M. Hurhangee, A. J. Kronemeijer, V. Pecunia, I. Nasrallah, I. Romanov, K. Broch, I. McCulloch, D. Emin, Y. Olivier, J. Cornil, D. Beljonne, H. Sirringhaus, Nature 2014, 515, 384.
[38] S. Ihnatsenka, X. Crispin, I. V. Zozoulenko, Physical Review B 2015, 92, 035201.
[39] D. Di Nuzzo, C. Fontanesi, R. Jones, S. Allard, I. Dumsch, U. Scherf, E. von Hauff, S. Schumacher, E. Da Como, Nat Commun 2015, 6.
[40] S. D. Baranovskii, I. P. Zvyagin, H. Cordes, S. Yamasaki, P. Thomas, physica status solidi (b) 2002, 230, 281.
[41] A. M. Glaudell, J. E. Cochran, S. N. Patel, M. L. Chabinyc, Advanced Energy Materials 2015, 5, n/a.
[42] N. Mateeva, H. Niculescu, J. Schlenoff, L. R. Testardi, J. Appl. Phys. 1998, 83, 3111.
[43] P. Bornoz, M. S. Prévot, X. Yu, N. Guijarro, K. Sivula, J. Am. Chem. Soc. 2015, 137, 15338.
[44] S. Fabiano, S. Braun, X. Liu, E. Weverberghs, P. Gerbaux, M. Fahlman, M. Berggren, X. Crispin, Adv. Mater. 2014, 26, 6000.
[45] F. Neese, J. Phys. Chem. Solids 2004, 65, 781.
[46] M. J. Frisch, G. W. Trucks, H. B. Schlegel, G. E. Scuseria, M. A. Robb, J. R. Cheeseman, G. Scalmani, V. Barone, B. Mennucci, G. A. Petersson, H. Nakatsuji, M. Caricato, X. Li, H. P. Hratchian, A. F. Izmaylov, J. Bloino, G. Zheng, J. L. Sonnenberg, M. Hada, M. Ehara, K. Toyota, R. Fukuda, J. Hasegawa, M. Ishida, T. Nakajima, Y. Honda, O. Kitao, H. Nakai, T. Vreven, J. A. Montgomery Jr., J. E. Peralta, F. É. ß. Ogliaro, M. J. Bearpark, J. Heyd, E. N. Brothers, K. N. Kudin, V. N. Staroverov, R. Kobayashi, J. Normand, K. Raghavachari, A. P. Rendell, J. C. Burant, S. S. Iyengar, J. Tomasi, M. Cossi, N. Rega, N. J. Millam, M. Klene, J. E. Knox, J. B. Cross, V.

Bakken, C. Adamo, J. Jaramillo, R. Gomperts, R. E. Stratmann, O. Yazyev, A. J. Austin, R. Cammi, C. Pomelli, J. W. Ochterski, R. L. Martin, K. Morokuma, V. G. Zakrzewski, G. A. Voth, P. Salvador, J. J. Dannenberg, S. Dapprich, A. D. Daniels, É. Ä. É. n. Farkas, J. B. Foresman, J. V. Ortiz, J. Cioslowski, D. J. Fox, *Gaussian 09, Revision D.01*, Gaussian, Inc., Wallingford, CT, USA 2009.

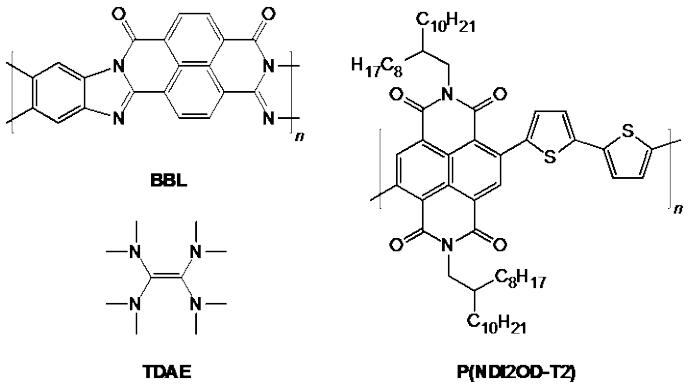

Scheme 1. Chemical structure of BBL, P(NDI2OD-T2) and TDAE.

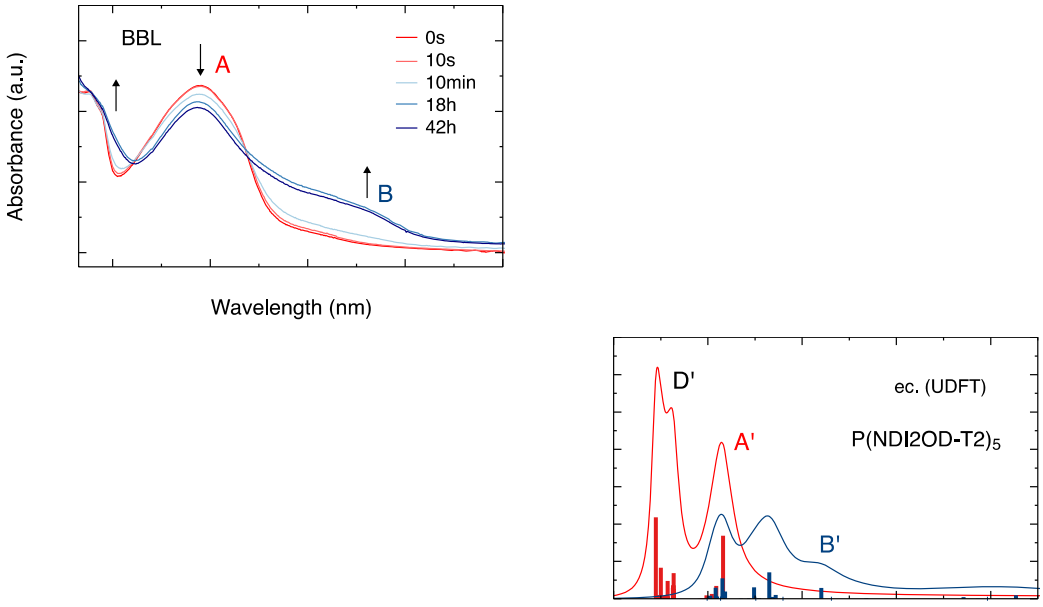

Figure 1. Experimental (*left*) and calculated (*right*) UV-Vis-NIR absorption spectra of BBL (a,c) and P(NDI2OD-T2) (b,d) films for different TDAE exposure times (panels a,b) and for neutral and charged electronic states (panels c,d).

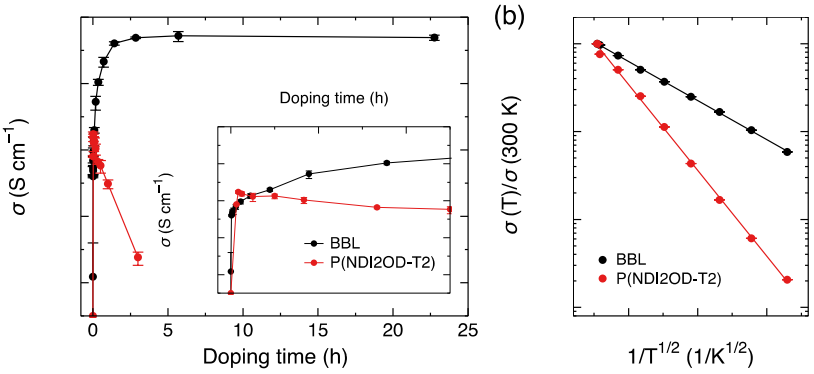

Figure 2. (a) Electrical conductivity of BBL and P(NDI2OD-T2) films as a function of the TDAE exposure time (doping time). (b) Temperature dependence of the electrical conductivity (normalized to 300 K) for doped BBL and P(NDI2OD-T2) samples.

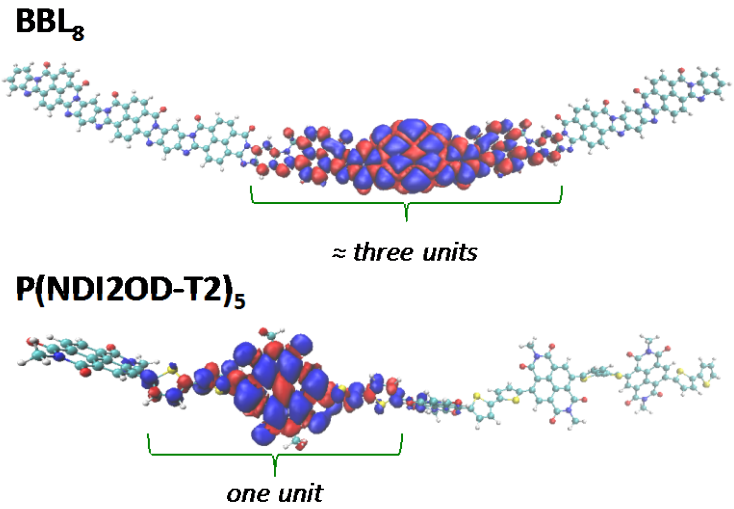

Figure 3. Spin (α and β) density distributions of the longest BBL (*n* = 8, *left*) and P(NDI2OD-T2) (*n* = 5, *right*) oligomers, as calculated at the UDFT-BS and UDFT level respectively (ωB97X-D3/6-31G*).

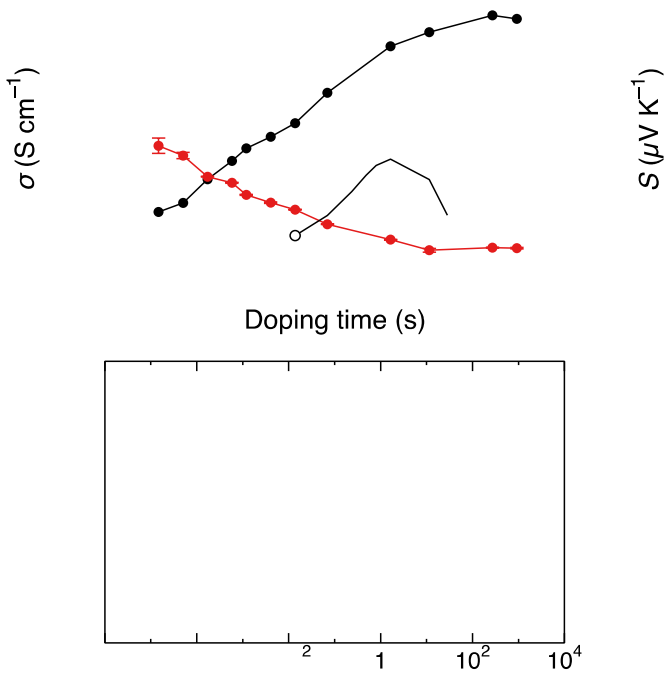

Figure 4. (a) Electrical conductivity σ and Seebeck coefficient S versus TDAE doping time for BBL and P(NDI2OD-T2) films. (b) Seebeck vs conductivity data for BBL and P(NDI2OD-T2). The dashed line indicates the empirical fit $S \propto \sigma^{-1/4}$ as extracted from Ref. [41].

Ladder-type '*torsion-free*' conducting polymers (e.g. BBL) can outperform '*structurally distorted*' donor-acceptor polymers (e.g. P(NDI2OD-T2)), in terms of conductivity and thermoelectric power factor. The polaron delocalization length is larger in BBL than in P(NDI2OD-T2), resulting in a higher measured polaron mobility. Structure-function relationships are drawn, setting material-design guidelines for the next-generation of conducting thermoelectric polymers.

Ladder-type conducting polymers

Suhao Wang, Hengda Sun, Ujwala Ail, Mikhail Vagin, Per O. Å. Persson, Jens W. Andreasen, Walter Thiel, Magnus Berggren, Xavier Crispin, Daniele Fazzi,* Simone Fabiano*

Thermoelectric properties of solution-processed n-doped ladder-type conducting polymers

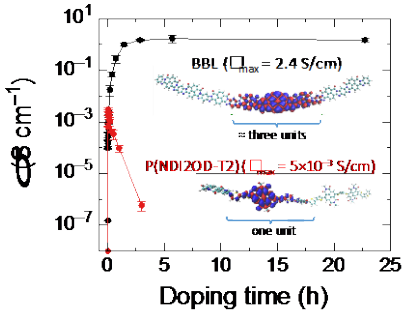

WILEY-VCH

Supporting Information

Thermoelectric properties of solution-processed n-doped ladder-type conducting polymers

Suhao Wang, Hengda Sun, Ujwala Ail, Mikhail Vagin, Per O. Å. Persson, Jens W. Andreasen, Walter Thiel, Magnus Berggren, Xavier Crispin, Daniele Fazzi, Simone Fabiano**

Dr. S. Wang, Dr. H. Sun, Dr. U. Ail, Prof. M. Berggren, Prof. X. Crispin, Dr. S. Fabiano
Laboratory of Organic Electronics, Department of Science and Technology, Linköping University, SE-60174, Norrköping, Sweden.
E-mail: simone.fabiano@liu.se

Prof. Per O. Å. Persson
Thin Film Physics Division, Department of Physics Chemistry and Biology, Linköping University, SE-581 83 Linköping, Sweden.

Dr. J. W. Andreasen
Technical University of Denmark, Department of Energy Conversion and Storage, Frederiksborgvej 399, 4000 Roskilde, Denmark.

Prof. W. Thiel, Dr. D. Fazzi
Max-Planck-Institut für Kohlenforschung, Kaiser-Wilhelm-Platz 1, D-45470 Mülheim an der Ruhr, Germany.
E-mail: fazzi@mpi-muelheim.mpg.de

Cyclic voltammetry

A BioLogic SP200 potentiostat was used for the electrochemical measurements with the three electrode setup. 0.1 M tetrabutylammonium hexafluoroborate (TBAP) in dry acetonitrile was utilized as a supporting electrolyte. Platinum disk (diam. 1 mm) and platinum wire were used as reference electrode and counter electrode, respectively. An Ag/Ag^+ quasi-reference electrode (QRE) was used (0.01 M $AgNO_3$ in 0.1 M TBAP). After each experiment, the system was calibrated by measuring the ferrocene/ferrocenium (Fc/Fc^+) redox potential, which was +0.096 V with respect to QRE. All measurements were carried out in a glove box under dry nitrogen.

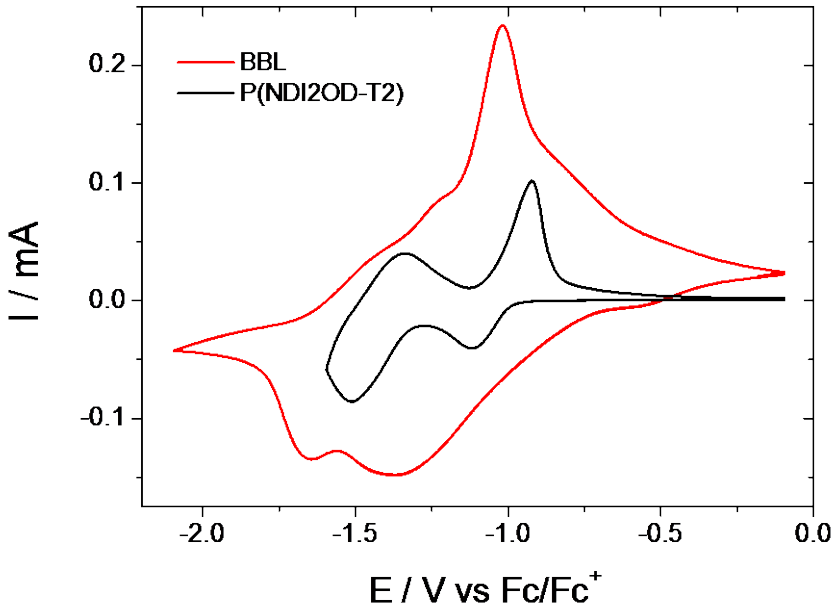

Figure S1. Cyclic voltammograms of P(NDI2OD-T2) and BBL (scan rate 20 mV/s).

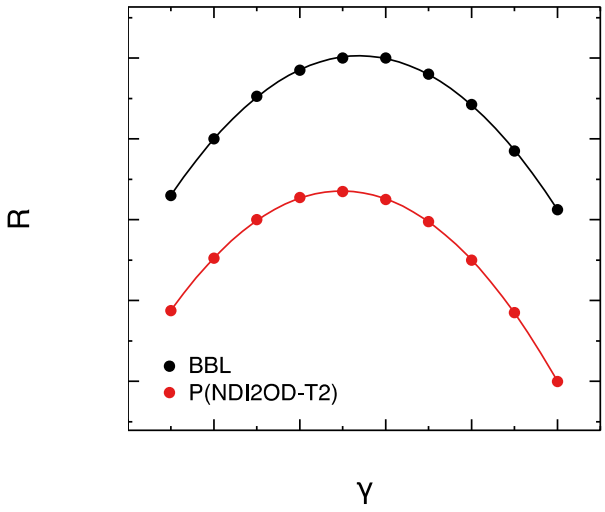

Figure S2. Evaluation of the Mott variable-range hopping exponent.

Structural charaterization

GIWAXS experimental: The silicon substrate surface was aligned at a grazing incident angle of 0.18° with respect to the incoming X-ray beam, supplied by a rotating Cu anode operated at 50 kV, 200 mA in point focus mode. The Cu k-alfa radiation (wavelength (λ) = 1.542 Å) was collimated and monochromatized with a 1D multilayer optic. The scattered radiation was recorded in vacuum on photo-stimulable imaging plates 121.5 mm from the sample. For further details of the instrumental setup, please refer to [Apitz, D., Bertram, R.P., Benter, N., Hieringer, W., Andreasen, J.W., Nielsen, M.M., Johansen, P.M., and Buse, K., 2005, Investigation of chromophore-chromophore interaction by electro-optic measurements, linear dichroism, x-ray scattering, and density-functional calculations: Physical Review E, v. 72, no. 3, p. 036610, 10 p.]. The data integration and conversion to reciprocal space coordinates was done with Matlab scripts described in [Breiby, D.W., Bunk, O., Andreasen, J.W., Lemke, H.T., and Nielsen, M.M., 2008, Simulating X-ray diffraction of textured films: Journal of Applied Crystallography, v. 41, no. Part 2, p. 262–271.]

TEM experimental: Electron microscopy was performed using the Linköping double corrected FEI Titan^3 G2 60-300. Images were recorded at low accelerating voltage (60 kV) to reduce knock on damage to the material and in monochromated TEM mode, with a beam limiting slit inserted in the first condenser image plane to reduce beam current to ~1 nA. The energy spread in monochromated mode was ¨150 mev (FWHM) which significantly reduces the impact of chromatic aberration (Cc) and extends the point resolution for lattice resolved imaging (<1.3Å). The samples were imaged in plan-view geometry.

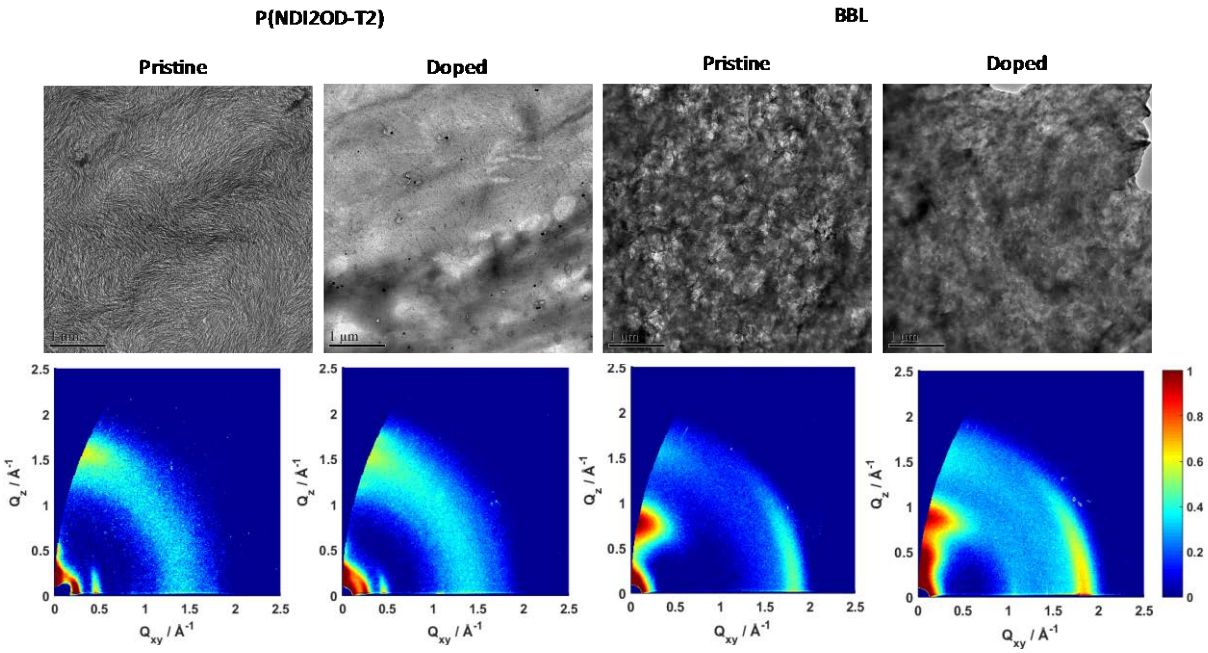

Figure S3. TEM images and GIWAXS patterns of pristine and doped P(NDI2OD-T2) and BBL.

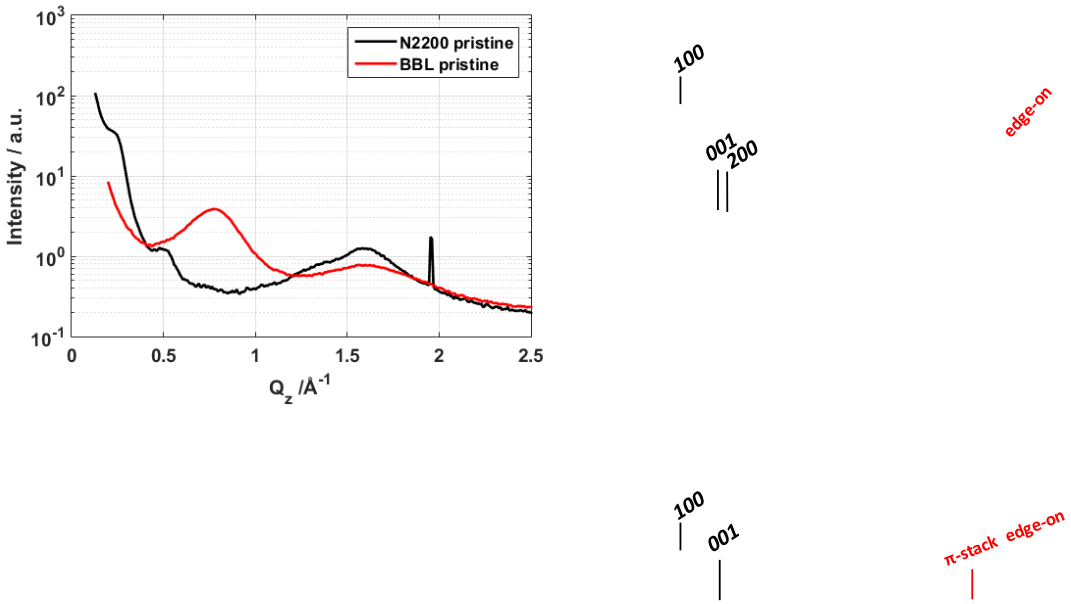

Figure S4. GIWAXS line cuts for pristine and doped P(NDI2OD-T2) [N2200] and BBL along the q_{xy} and q_z axes.

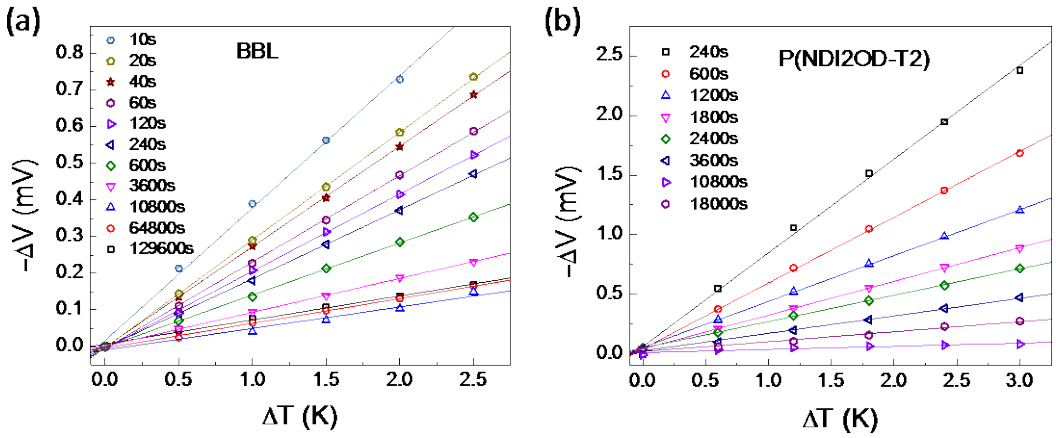

Figure S5. Thermal voltage as a function of ΔT for BBL (a) and P(NDI2OD-T2) (b) films for different TDAE doping time. The error bar in the final Seebeck coefficient values is obtained from the standard linear fitting error.

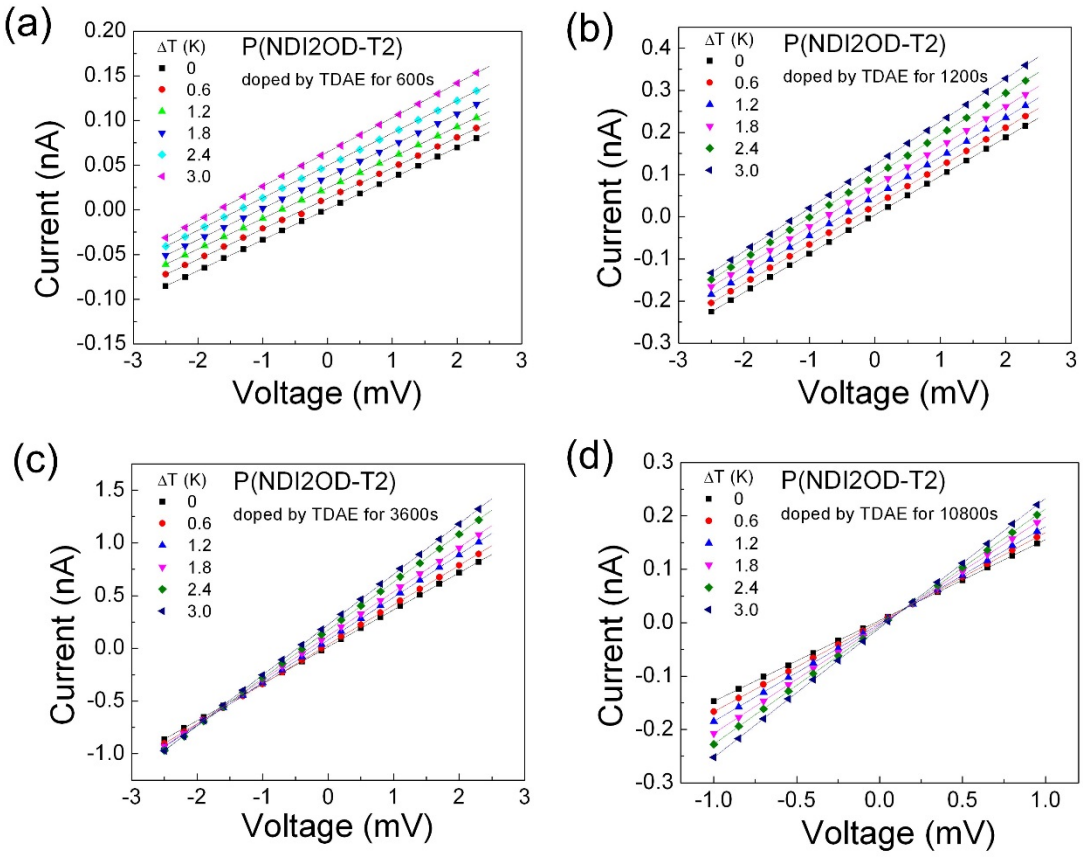

Figure S6. Current-voltage (I-V) curves for P(NDI2OD-T2) films doped by TDAE for different time. For (a) 600s, and (b) 1200s when the samples are not saturated, the slopes remain roughly same with increasing ΔT, whereas for (c) 3600s and (d) 10800s when the samples are saturated or oversaturated, the slopes changes with increasing ΔT.

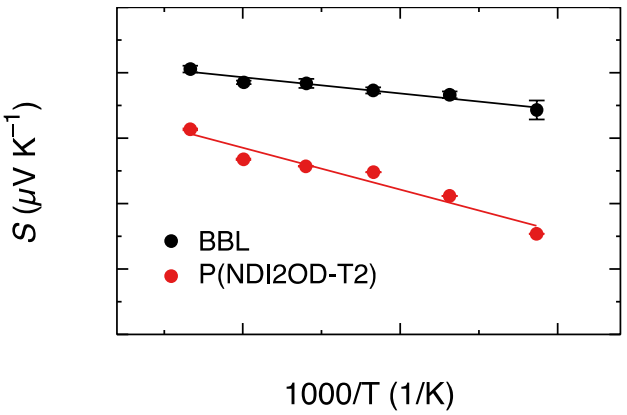

Figure S7. Temperature dependence of Seebeck coefficient for doped BBL and P(NDI2OD-T2) films.

Computational results

Computed TDDFT (ωB97X-D3/6-31G*) vertical excitation energies (eV) and oscillator strengths for the longest oligomers of BBL (n=8) and P(NDI2OD-T2) (n = 5) in their neutral and charged states, respectively.

BBL, n = 8 ωB97X-D/6-31G* *Neutral state*	Energy eV	Oscillator Strength
S1	**2.7701**	**9.1965**
S2	2.8335	0.5543
S3	2.8991	0.4547
S4	2.9525	0.0617
S5	2.9909	0.0847
S6	3.0157	0.0125
S7	3.0289	0.0162
S8	3.0358	0.0011
S9	3.5222	0.3993
S10	3.5340	0.0227

BBL, n = 8 UωB97X-D/6-31G* *Charged (-1) state*	Energy eV	Oscillator Strength
D1	*-0.1610*	*-0.0094*
D2	*-0.1188*	*-0.0016*
D3	*-0.0467*	*-0.0777*
D4	0. 2645	0.0032
D5	0.2647	0.0022
D6	0.3134	0.0000
D7	0.3137	0.0000
D8	1.5554	0.0362
D9	1.6578	0.0000
D10	1.6621	0.0057

BBL, n = 8 UωB97X-D/6-31G* **broken symmetry (BS)** *Charged (-1) state*	Energy eV	Oscillator Strength
D1	1.1460	0.0039
D2	1.1680	0.0094
D3	1.1922	0.0002
D4	1.2375	0.0000
D5	1.2439	0.0000
D6	1.2711	0.0001
D7	1.2878	0.0001
D8	1.5891	0.0001
D9	1.5901	0.0001
D10	1.6697	0.0000
D11	1.6749	0.0000
D12	1.6930	0.0000
D13	1.7113	0.0000
D14	1.7228	0.0000

D15	1.9209	0.0277
D16	2.1614	0.6552
D17	2.4079	0.4653
D18	2.4228	0.0035
D19	**2.4980**	**3.5809**
D20	2.5840	0.0380

P(NDI2OD-T2), n = 5 ωB97X-D/6-31G* *Neutral state*	Energy eV	Oscillator Strength
S1	**2.8699**	**1.6842**
S2	2.9668	0.3425
S3	2.9881	0.0690
S4	3.0353	0.1274
S5	3.1241	0.0901
S6	3.1673	0.0058
S7	3.1865	0.0065
S8	3.2017	0.0106
S9	3.2411	0.0033
S10	3.7903	0.6863

P(NDI2OD-T2), n = 5 UωB97X-D/6-31G* *Charged (-1) state*	Energy eV	Oscillator Strength
D1	1.1769	0.0896
D2	1.2498	0.0007
D3	1.2745	0.0026
D4	1.3156	0.0396
D5	1.6840	0.0112
D6	1.8752	0.0010
D7	**1.9361**	**0.2908**
D8	2.0471	0.0000
D9	2.0691	0.0000
D10	2.2204	0.0005
D11	2.2803	0.0988
D12	2.3114	0.0498
D13	**2.3385**	**0.7057**
D14	2.4377	0.0169
D15	2.4778	0.0008
D16	2.4896	0.3026
D17	2.5431	0.0085
D18	2.5680	0.0000
D19	2.5806	0.0000

Computed DFT energy difference ΔE = E(UDFT-BS) – E(UDFT) between the unrestricted (UDFT) and the unrestricted – broken symmetry (UDFT-BS) solution for the BBL and P(NDI2OD-T2) oligomers investigated.

	BBL_n				$P(NDI2OD-T2)_n$
n	1	2	4	8	5
ΔE / eV	0.00	0.00	-0.27	-0.42	0.00

Comparison between the computed polaron structural relaxations (i.e. bond length difference) for BBL_8 (UDFT-BS) and $P(NDI2OD\text{-}T2)_5$ (UDFT). Bond length difference is computed as the difference between each bond in the charged and in the neutral state.

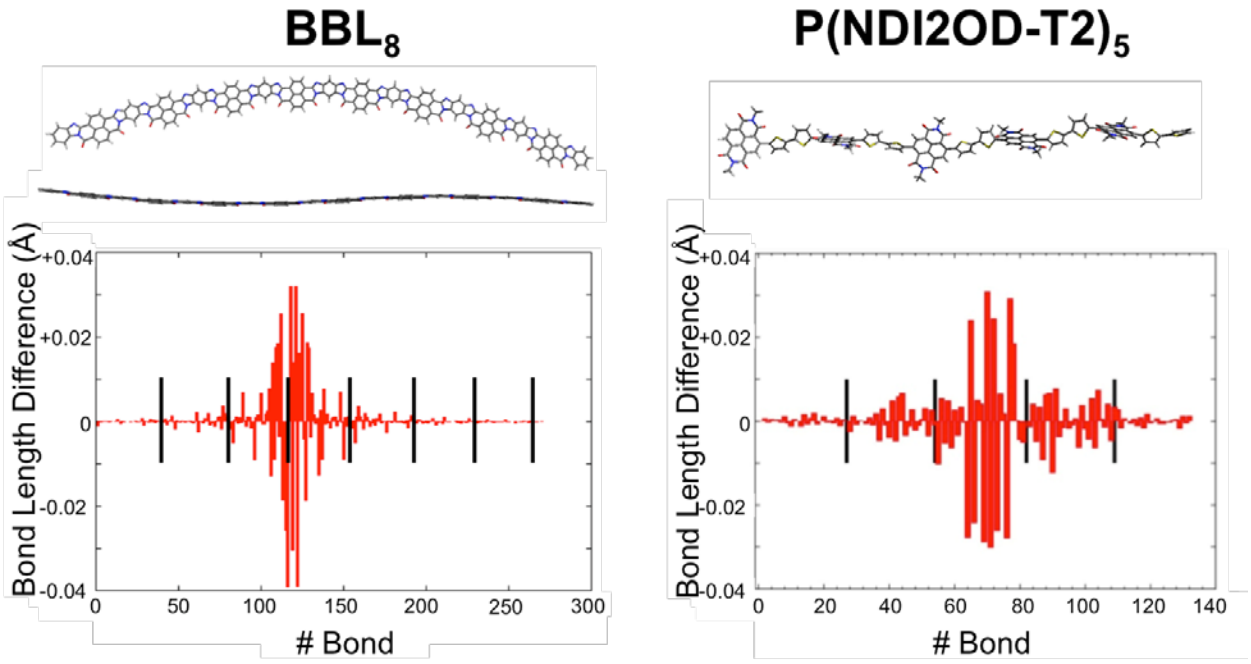

Comparison between the computed polaron structural relaxations at the UDFT and UDFT-BS levels, for BBL_4 and BBL_8. Structural relaxations are evaluated as bond length differences (Å) between the charged and the neutral optimized structures (C-H bonds are omitted from the analysis).

BBL_4 - *UDFT*	BBL_4 – *UDFT-BS*
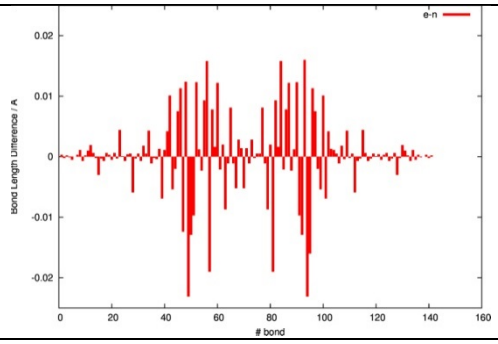	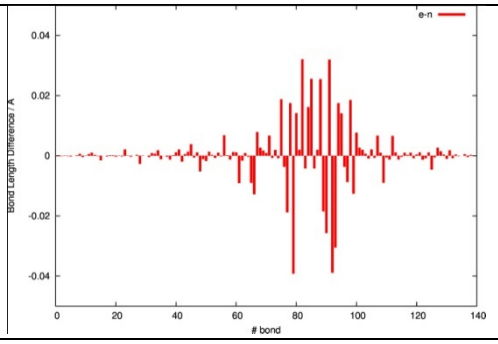
BBL_8 - *UDFT*	BBL_8 – *UDFT-BS*
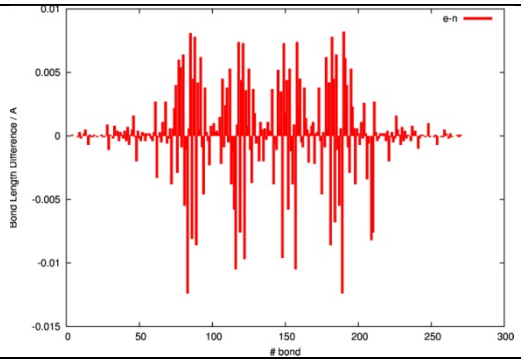	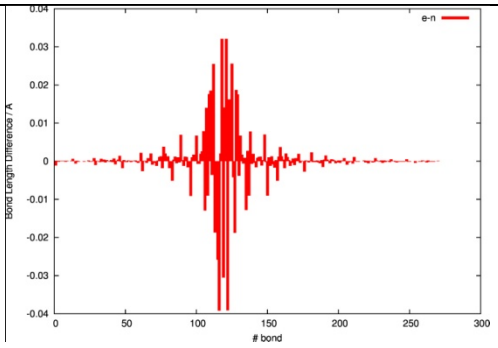

DFT optimized molecular structures: Cartesian coordinates (Å)

BBL, n = 1, ωB97X-D/6-31G*, neutral state

C	-2.555280	3.432870	0.189904
C	-3.178680	2.120154	0.142830
C	-2.332278	0.991721	-0.023268
C	-0.923379	1.129248	-0.140545
C	-0.276879	2.470689	-0.093445
N	-1.164064	3.533226	0.071632
C	-2.904131	-0.299942	-0.073322
C	-4.312601	-0.441057	0.043543
C	-5.112169	0.672077	0.204175
C	-4.544179	1.955020	0.253909
C	-2.054748	-1.426253	-0.239519
C	-2.613068	-2.806275	-0.297766
N	-4.000321	-2.872930	-0.177469
C	-4.865273	-1.784712	-0.012490
C	-0.122920	0.019991	-0.300953
C	-0.691536	-1.264354	-0.350709
O	-1.935230	-3.801833	-0.438661
C	-4.811241	-4.010340	-0.193870
O	0.919329	2.645736	-0.187775
C	-0.867993	4.896092	0.152481
H	-5.170728	2.831510	0.380103
H	-6.185320	0.539806	0.291258
H	0.949612	0.156591	-0.387733
H	-0.068591	-2.143321	-0.476742
N	-6.113638	-2.129924	0.073969
C	-6.117062	-3.516928	-0.035770
N	-3.142213	4.581709	0.333798
C	-2.115719	5.520762	0.314877
C	-2.194821	6.908072	0.431544
C	-1.009778	7.627788	0.380981
C	0.228462	6.985669	0.218119
C	0.327391	5.604626	0.100134
H	1.275959	5.099433	-0.025708
H	1.134147	7.583169	0.183229
H	-1.037632	8.709339	0.468866
H	-3.156425	7.393824	0.557009
C	-7.199423	-4.395807	-0.006828
C	-4.529587	-5.365629	-0.327159
C	-5.620663	-6.225549	-0.296006
C	-6.933029	-5.750921	-0.138761
H	-8.208938	-4.018487	0.115153
H	-7.753898	-6.460915	-0.120342
H	-5.452408	-7.293336	-0.396107
H	-3.514429	-5.720211	-0.447793

E = -1367.10698241 Hartree

BBL, n = 1, ωB97X-D/6-31G*, charged (-1) state

C	-2.571524	3.419096	0.190382
C	-3.180586	2.118018	0.142814
C	-2.329734	0.999484	-0.022974
C	-0.917873	1.140394	-0.140083
C	-0.285550	2.444686	-0.094307
N	-1.184946	3.518447	0.072305
C	-2.908170	-0.307009	-0.073793
C	-4.312311	-0.438176	0.043407
C	-5.128959	0.693220	0.207119
C	-4.571172	1.953078	0.256100
C	-2.059336	-1.437782	-0.240386
C	-2.599758	-2.782313	-0.297694
N	-4.003461	-2.847643	-0.175280
C	-4.866043	-1.763480	-0.011102
C	-0.108736	-0.002901	-0.304056
C	-0.664994	-1.259299	-0.352934
O	-1.948515	-3.814149	-0.438365
C	-4.806078	-3.983296	-0.192122
O	0.919478	2.663739	-0.186578
C	-0.884616	4.874031	0.152186
H	-5.187219	2.837356	0.382020
H	-6.200802	0.547998	0.293020
H	0.963098	0.141429	-0.390005
H	-0.048296	-2.142966	-0.478883
N	-6.130555	-2.118348	0.075806
C	-6.119329	-3.494102	-0.034037
N	-3.162191	4.586270	0.336306
C	-2.134226	5.507006	0.315729
C	-2.192470	6.899562	0.431113
C	-1.003352	7.612401	0.379462
C	0.231617	6.962434	0.215908
C	0.313981	5.579894	0.099128
H	1.253834	5.058951	-0.027419
H	1.143366	7.552528	0.179748
H	-1.025545	8.695634	0.467116
H	-3.150422	7.394517	0.557252
C	-7.191493	-4.391700	-0.007557
C	-4.520268	-5.339119	-0.325351
C	-5.601289	-6.212262	-0.296128
C	-6.917256	-5.745281	-0.139550
H	-8.205438	-4.023245	0.113772
H	-7.735657	-6.460453	-0.121709
H	-5.423305	-7.279504	-0.396724
H	-3.499271	-5.676751	-0.444884

E = -1367.18798960 Hartree

BBL, n = 2, ωB97X-D/6-31G*, neutral state

C	13.403365	-0.860643	-0.000263
C	12.316794	-1.723108	0.000685
C	11.041741	-1.158280	0.000232
C	10.887036	0.238031	-0.001122
C	11.967148	1.114083	-0.002109
C	13.229482	0.532833	-0.001656
N	9.805069	-1.795087	0.001014
C	8.929384	-0.837054	0.000190
N	9.504086	0.438979	-0.001138
C	7.481656	-0.964874	0.000490
C	6.712406	0.228911	-0.000225
C	7.326712	1.509831	-0.001345
C	8.810713	1.648918	-0.001902
C	6.858268	-2.195968	0.001465
C	5.457504	-2.283158	0.001698
C	4.686542	-1.138423	0.001047
C	5.302024	0.141169	0.000138
C	4.534216	1.336164	-0.000418
C	3.045173	1.291515	0.000066
N	2.505646	0.004635	0.000922
C	3.234111	-1.191397	0.001119

C	1.157178	-0.360094	0.000909
C	1.176472	-1.777657	0.001239
N	2.485008	-2.249758	0.001290
C	6.558111	2.652991	-0.001949
C	5.155021	2.565628	-0.001435
C	0.000035	-2.517219	0.001262
C	-1.176389	-1.777667	0.000958
C	-1.157178	-0.360088	0.000722
C	0.000015	0.407253	0.000702
O	2.341203	2.278238	-0.000190
O	9.387137	2.715652	-0.003009
N	-2.484970	-2.249794	0.000609
C	-3.234112	-1.191452	0.000622
C	-4.686552	-1.138486	0.000279
C	-5.302029	0.141109	0.000875
C	-4.534205	1.336095	0.001607
C	-3.045195	1.291453	0.001510
N	-2.505615	0.004544	0.000727
C	-5.457541	-2.283205	-0.000581
C	-6.858303	-2.195994	-0.000915
C	-7.481676	-0.964896	-0.000315
C	-6.712408	0.228877	0.000684
C	-7.326699	1.509810	0.001519
C	-8.810698	1.648923	0.001484
N	-9.504085	0.438984	0.000312
C	-8.929401	-0.837052	-0.000850
C	-10.887036	0.238057	-0.000696
C	-11.041759	-1.158252	-0.002368
N	-9.805097	-1.795075	-0.002376
C	-5.154998	2.565572	0.002347
C	-6.558088	2.652956	0.002363
C	-12.316819	-1.723069	-0.003896
C	-13.403378	-0.860596	-0.003641
C	-13.229479	0.532880	-0.001867
C	-11.967142	1.114117	-0.000357
O	-9.387114	2.715657	0.002324
O	-2.341278	2.278218	0.002157
H	-7.468234	-3.093094	-0.001669
H	-4.963432	-3.248852	-0.001004
H	-7.054183	3.617435	0.003005
H	-4.542376	3.460772	0.002901
H	-11.823259	2.186437	0.001043
H	-14.104055	1.176031	-0.001680
H	-14.409253	-1.268793	-0.004868
H	-12.438894	-2.800757	-0.005306
H	4.963390	-3.248803	0.002392
H	7.468184	-3.093078	0.002011
H	4.542400	3.460828	-0.001838
H	7.054214	3.617465	-0.002832
H	-0.000003	1.486774	0.000606
H	0.000062	-3.600490	0.001341
H	12.438864	-2.800797	0.001806
H	14.409236	-1.268850	0.000076
H	14.104066	1.175974	-0.002368
H	11.823266	2.186403	-0.003194

E = -2502.04817843 Hartree

BBL, n = 2, ωB97X-D/6-31G*, charged (-1) state

C	13.390000	-0.837450	0.000203
C	12.308804	-1.706844	0.000326
C	11.025454	-1.156143	0.000068
C	10.862514	0.241919	-0.000298
C	11.938956	1.123770	-0.000442
C	13.207212	0.555138	-0.000181
N	9.799614	-1.801266	0.000140
C	8.912367	-0.840924	-0.000136
N	9.482297	0.434714	-0.000482
C	7.473007	-0.965492	-0.000114
C	6.708227	0.228092	-0.000222
C	7.321769	1.510995	-0.000491
C	8.782898	1.652422	-0.000801
C	6.845334	-2.207823	0.000100
C	5.457400	-2.296755	0.000188
C	4.679806	-1.141817	0.000128
C	5.290149	0.137946	-0.000054
C	4.516154	1.331020	-0.000068
C	3.046576	1.288334	0.000185
N	2.507418	-0.001197	0.000290
C	3.236045	-1.195820	0.000201
C	1.160093	-0.365575	0.000281
C	1.179719	-1.786036	0.000261
N	2.481783	-2.260690	0.000192
C	6.534915	2.660961	-0.000513
C	5.147837	2.572986	-0.000300
C	0.000001	-2.523111	0.000265
C	-1.179717	-1.786035	0.000303
C	-1.160091	-0.365574	0.000367
C	0.000001	0.398280	0.000351
O	2.326091	2.275059	0.000019
O	9.384030	2.714576	-0.000646
N	-2.481782	-2.260688	0.000243
C	-3.236044	-1.195819	0.000326
C	-4.679805	-1.141817	0.000239
C	-5.290149	0.137946	0.000338
C	-4.516154	1.331020	0.000588
C	-3.046575	1.288334	0.000852
N	-2.507417	-0.001196	0.000481
C	-5.457400	-2.296753	-0.000020
C	-6.845334	-2.207822	-0.000177
C	-7.473007	-0.965492	-0.000096
C	-6.708227	0.228092	0.000163
C	-7.321770	1.510995	0.000255
C	-8.782899	1.652421	0.000044
N	-9.482298	0.434714	-0.000096
C	-8.912368	-0.840924	-0.000266
C	-10.862515	0.241919	-0.000276
C	-11.025455	-1.156143	-0.000594
N	-9.799614	-1.801265	-0.000585
C	-5.147837	2.572985	0.000654
C	-6.534916	2.660960	0.000505
C	-12.308804	-1.706845	-0.000887
C	-13.390001	-0.837451	-0.000841
C	-13.207213	0.555137	-0.000503
C	-11.938957	1.123769	-0.000217
O	-9.384030	2.714575	0.000401
O	-2.326092	2.275060	0.000497
H	-7.461403	-3.100973	-0.000382
H	-4.958186	-3.259728	-0.000102
H	-7.032581	3.624885	0.000576
H	-4.528689	3.463497	0.000858

H	-11.781142	2.194200	0.000040
H	-14.076918	1.205832	-0.000476
H	-14.399069	-1.240019	-0.001078
H	-12.439593	-2.784045	-0.001160
H	4.958186	-3.259730	0.000330
H	7.461403	-3.100974	0.000191
H	4.528689	3.463498	-0.000307
H	7.032580	3.624886	-0.000730
H	0.000001	1.477628	0.000420
H	0.000001	-3.606822	0.000214
H	12.439594	-2.784045	0.000631
H	14.399069	-1.240017	0.000405
H	14.076917	1.205833	-0.000278
H	11.781140	2.194201	-0.000755

E = -2502.12481349 Hartree

BBL, n = 4, ωB97X-D/6-31G*, neutral state

C	-0.000007	-0.556437	0.691381
C	1.157124	-1.313114	0.564324
C	1.176518	-2.712009	0.335018
C	-0.000009	-3.442367	0.219253
C	-1.176525	-2.712008	0.335049
C	-1.157141	-1.313110	0.564336
N	2.484981	-3.173907	0.236178
C	3.233497	-2.126356	0.389912
N	2.505106	-0.949065	0.600191
C	4.685040	-2.064996	0.345675
C	5.298763	-0.795283	0.511434
C	4.531340	0.379690	0.730976
C	3.043723	0.324811	0.786509
C	6.707107	-0.695948	0.450520
C	7.475493	-1.868896	0.226210
C	6.854383	-3.091866	0.074638
C	5.455663	-3.190295	0.134197
C	7.319262	0.575978	0.609170
C	8.799508	0.729475	0.536805
N	9.492622	-0.459202	0.304686
C	8.920001	-1.727822	0.152683
C	10.871796	-0.635674	0.170546
C	11.028265	-2.026534	-0.053488
N	9.792174	-2.664496	-0.055289
C	11.920728	0.272803	0.218802
C	13.159794	-0.321574	0.020495
C	13.354019	-1.707520	-0.206328
C	12.282996	-2.591926	-0.245584
N	14.704881	-1.991400	-0.377408
C	15.313696	-0.852113	-0.265245
N	14.447019	0.219756	-0.019454
C	16.740866	-0.601787	-0.373418
C	17.191758	0.735608	-0.218202
C	16.287249	1.800871	0.036445
C	14.822047	1.553875	0.147221
C	18.573389	1.014051	-0.321466
C	19.478094	-0.049271	-0.580349
C	19.013196	-1.340346	-0.726841
C	17.641623	-1.617182	-0.622381
C	19.024159	2.352081	-0.164723
C	20.472480	2.690857	-0.265399
N	21.303902	1.601374	-0.524501
C	20.890857	0.273986	-0.685879
C	22.692924	1.593057	-0.680809
C	23.013079	0.247407	-0.927549
N	21.869714	-0.544454	-0.923221
C	23.653831	2.597043	-0.631488
C	24.969011	2.200418	-0.842727
C	25.307411	0.860280	-1.091493
C	24.338820	-0.131454	-1.137224
C	16.750911	3.089568	0.184292
C	18.125671	3.366050	0.083862
C	5.150486	1.599876	0.888180
C	6.551512	1.698797	0.826473
O	20.911916	3.813610	-0.137645
O	14.005566	2.423602	0.361638
O	9.374173	1.789229	0.662248
O	2.339747	1.294112	0.970681
N	-2.484994	-3.173915	0.236274
C	-3.233503	-2.126370	0.390019
N	-2.505112	-0.949069	0.600246
C	-3.043724	0.324804	0.786598
C	-4.531341	0.379685	0.731079
C	-5.298769	-0.795292	0.511568
C	-4.685049	-2.065007	0.345812
C	-6.707113	-0.695957	0.450675
C	-7.475503	-1.868909	0.226390
C	-6.854397	-3.091880	0.074819
C	-5.455675	-3.190307	0.134357
C	-7.319268	0.575971	0.609316
C	-6.551515	1.698794	0.826579
C	-5.150487	1.599874	0.888267
C	-8.799517	0.729460	0.537011
N	-9.492631	-0.459214	0.304865
C	-8.920011	-1.727834	0.152866
N	-9.792187	-2.664511	-0.055086
C	-11.028274	-2.026544	-0.053305
C	-10.871801	-0.635678	0.170684
C	-12.283007	-2.591938	-0.245392
C	-13.354025	-1.707527	-0.206175
C	-13.159797	-0.321573	0.020598
C	-11.920731	0.272805	0.218900
N	-14.447020	0.219759	-0.019380
C	-15.313699	-0.852115	-0.265140
N	-14.704887	-1.991411	-0.377248
C	-14.822047	1.553886	0.147241
C	-16.287244	1.800886	0.036412
C	-17.191754	0.735616	-0.218202
C	-16.740865	-0.601789	-0.373345
C	-18.573380	1.014060	-0.321513
C	-19.478085	-0.049270	-0.580359
C	-19.013191	-1.340356	-0.726773
C	-17.641621	-1.617192	-0.622276
C	-19.024148	2.352101	-0.164845
C	-18.125661	3.366076	0.083714
C	-16.750903	3.089593	0.184183
C	-20.472464	2.690881	-0.265588
N	-21.303888	1.601385	-0.524628
C	-20.890846	0.273986	-0.685924
N	-21.869702	-0.544464	-0.923232
C	-23.013066	0.247399	-0.927602
C	-22.692909	1.593062	-0.680935
C	-24.338807	-0.131472	-1.137259

C	-25.307397	0.860266	-1.091585
C	-24.968995	2.200417	-0.842895
C	-23.653814	2.597052	-0.631675
O	-2.339750	1.294111	0.970741
O	-9.374173	1.789233	0.662328
O	-14.005557	2.423634	0.361541
O	-20.911909	3.813625	-0.137786
H	-19.724862	-2.134721	-0.924477
H	-17.271077	-2.630128	-0.738123
H	-18.498811	4.377936	0.199933
H	-16.037237	3.883136	0.377977
H	-23.385150	3.627335	-0.439915
H	-25.754356	2.949096	-0.814920
H	-26.348935	0.599554	-1.251461
H	-24.586696	-1.169942	-1.327985
H	-7.463565	-3.972930	-0.096293
H	-4.963110	-4.148595	0.009210
H	-7.046365	2.656652	0.945125
H	-4.538525	2.479619	1.055637
H	-11.785026	1.330217	0.388388
H	-12.417724	-3.652432	-0.419733
H	4.963098	-4.148583	0.009053
H	7.463548	-3.972917	-0.096485
H	4.538524	2.479617	1.055573
H	7.046366	2.656653	0.945021
H	0.000004	0.509386	0.862621
H	-0.000002	-4.510566	0.039291
H	17.271077	-2.630110	-0.738287
H	19.724866	-2.134705	-0.924571
H	16.037244	3.883103	0.378114
H	18.498824	4.377902	0.200136
H	11.785025	1.330211	0.388319
H	12.417710	-3.652413	-0.419964
H	24.586709	-1.169913	-1.328011
H	26.348948	0.599574	-1.251383
H	25.754374	2.949093	-0.814707
H	23.385166	3.627314	-0.439668

E = -4771.93058488 Hartree

BBL, n = 4, UωB97X-D/6-31G*, charged (-1) state

C	0.000001	-0.580836	0.678295
C	1.159940	-1.334317	0.552541
C	1.179567	-2.736127	0.323679
C	0.000000	-3.464328	0.208890
C	-1.179566	-2.736126	0.323679
C	-1.159939	-1.334317	0.552541
N	2.481484	-3.200910	0.224718
C	3.235093	-2.147012	0.378101
N	2.506878	-0.970737	0.587624
C	4.677869	-2.085341	0.334168
C	5.287143	-0.815862	0.500673
C	4.514214	0.357503	0.719837
C	3.045393	0.305428	0.774028
C	6.703241	-0.714824	0.440203
C	7.466159	-1.888618	0.216241
C	6.839810	-3.122500	0.062286
C	5.454103	-3.221360	0.120574
C	7.314739	0.558714	0.599504
C	8.771699	0.713720	0.529600
N	9.470458	-0.484688	0.296188
C	8.901349	-1.752580	0.143342
C	10.845444	-0.653394	0.164807
C	11.009660	-2.047495	-0.060063
N	9.784992	-2.692376	-0.064735
C	11.890815	0.260790	0.215522
C	13.134612	-0.323525	0.019962
C	13.337211	-1.707228	-0.206658
C	12.272253	-2.599499	-0.248918
N	14.692094	-1.982309	-0.374758
C	15.294976	-0.840764	-0.261208
N	14.422515	0.227510	-0.017199
C	16.721827	-0.589355	-0.367209
C	17.171964	0.748924	-0.212362
C	16.261929	1.809182	0.039638
C	14.793055	1.556848	0.148647
C	18.553094	1.031492	-0.313226
C	19.460408	-0.029514	-0.569384
C	18.996799	-1.321659	-0.715535
C	17.626231	-1.602612	-0.613747
C	18.998072	2.371781	-0.156522
C	20.442474	2.714622	-0.254434
N	21.279116	1.626137	-0.511296
C	20.871972	0.296689	-0.672499
C	22.667842	1.624690	-0.664391
C	22.995052	0.280201	-0.909479
N	21.856395	-0.517610	-0.907192
C	23.624090	2.633120	-0.613811
C	24.942212	2.244012	-0.821945
C	25.287550	0.905604	-1.069047
C	24.323437	-0.090883	-1.116007
C	16.719476	3.099708	0.187403
C	18.093133	3.381498	0.089441
C	5.144265	1.589740	0.879162
C	6.529352	1.688637	0.818938
O	20.884044	3.837633	-0.127453
O	13.983282	2.433797	0.362209
O	9.373400	1.767286	0.652836
O	2.325901	1.274972	0.958078
N	-2.481483	-3.200909	0.224720
C	-3.235092	-2.147011	0.378103
N	-2.506877	-0.970736	0.587623
C	-3.045392	0.305429	0.774027
C	-4.514214	0.357503	0.719840
C	-5.287143	-0.815862	0.500678
C	-4.677869	-2.085340	0.334172
C	-6.703241	-0.714824	0.440211
C	-7.466160	-1.888619	0.216249
C	-6.839810	-3.122500	0.062292
C	-5.454103	-3.221360	0.120579
C	-7.314740	0.558713	0.599515
C	-6.529352	1.688636	0.818947
C	-5.144265	1.589739	0.879167
C	-8.771700	0.713718	0.529617
N	-9.470459	-0.484689	0.296199
C	-8.901350	-1.752580	0.143350
N	-9.784992	-2.692376	-0.064729
C	-11.009660	-2.047495	-0.060058
C	-10.845445	-0.653394	0.164813
C	-12.272253	-2.599498	-0.248915
C	-13.337211	-1.707228	-0.206656

C	-13.134613	-0.323524	0.019965
C	-11.890816	0.260790	0.215527
N	-14.422516	0.227510	-0.017197
C	-15.294976	-0.840763	-0.261208
N	-14.692094	-1.982308	-0.374757
C	-14.793056	1.556848	0.148648
C	-16.261929	1.809183	0.039635
C	-17.171964	0.748925	-0.212366
C	-16.721827	-0.589354	-0.367211
C	-18.553094	1.031493	-0.313233
C	-19.460407	-0.029513	-0.569389
C	-18.996798	-1.321659	-0.715538
C	-17.626231	-1.602612	-0.613748
C	-18.998071	2.371783	-0.156531
C	-18.093133	3.381499	0.089433
C	-16.719476	3.099709	0.187398
C	-20.442473	2.714624	-0.254451
N	-21.279115	1.626138	-0.511305
C	-20.871972	0.296689	-0.672503
N	-21.856395	-0.517611	-0.907192
C	-22.995052	0.280200	-0.909477
C	-22.667842	1.624690	-0.664394
C	-24.323438	-0.090886	-1.115999
C	-25.287551	0.905601	-1.069039
C	-24.942213	2.244010	-0.821942
C	-23.624090	2.633120	-0.613814
O	-2.325902	1.274973	0.958080
O	-9.373400	1.767286	0.652842
O	-13.983282	2.433798	0.362208
O	-20.884044	3.837634	-0.127458
H	-19.710524	-2.114868	-0.911336
H	-17.257185	-2.616017	-0.729550
H	-18.461241	4.395298	0.205703
H	-16.000322	3.888777	0.379028
H	-23.348132	3.661709	-0.423142
H	-25.723563	2.997041	-0.792709
H	-26.330766	0.649457	-1.226828
H	-24.576863	-1.128338	-1.305679
H	-7.454163	-4.000202	-0.108550
H	-4.955829	-4.176642	-0.004118
H	-7.025736	2.645800	0.938136
H	-4.526270	2.465063	1.046346
H	-11.741696	1.316069	0.385891
H	-12.416007	-3.658911	-0.423626
H	4.955829	-4.176643	-0.004121
H	7.454162	-4.000202	-0.108556
H	4.526271	2.465064	1.046342
H	7.025736	2.645801	0.938125
H	0.000001	0.484998	0.848350
H	0.000000	-4.532985	0.029165
H	17.257185	-2.616017	-0.729550
H	19.710525	-2.114868	-0.911335
H	16.000322	3.888776	0.379033
H	18.461242	4.395297	0.205714
H	11.741695	1.316070	0.385884
H	12.416007	-3.658912	-0.423629
H	24.576862	-1.128336	-1.305691
H	26.330764	0.649460	-1.226841
H	25.723562	2.997042	-0.792713
H	23.348132	3.661709	-0.423135

E = -4772.01136729 Hartree

BBL, n = 4, UωB97X-D/6-31G* broken symmetry (BS), charged (-1) state

C	-0.030736	-0.593289	0.673982
C	1.133815	-1.337918	0.552536
C	1.162160	-2.736389	0.325699
C	-0.008161	-3.478008	0.208115
C	-1.198730	-2.764535	0.317658
C	-1.185199	-1.357264	0.545233
N	2.475977	-3.188864	0.230346
C	3.219877	-2.138429	0.383662
N	2.485665	-0.963038	0.590518
C	4.669922	-2.080603	0.339663
C	5.287849	-0.811550	0.504307
C	4.515664	0.359399	0.721207
C	3.021239	0.302313	0.776401
C	6.696414	-0.711038	0.444727
C	7.464488	-1.883714	0.222934
C	6.840009	-3.106532	0.072277
C	5.442467	-3.206475	0.130408
C	7.304912	0.563121	0.602740
C	8.779818	0.718503	0.532473
N	9.476592	-0.472687	0.301791
C	8.907419	-1.743500	0.150532
C	10.854919	-0.643065	0.170290
C	11.017385	-2.034585	-0.051763
N	9.785491	-2.678081	-0.054818
C	11.900323	0.269779	0.218929
C	13.142571	-0.318931	0.023516
C	13.342958	-1.703349	-0.200745
C	12.275411	-2.592980	-0.240674
N	14.696301	-1.981408	-0.369114
C	15.300322	-0.839911	-0.257829
N	14.429021	0.229016	-0.015251
C	16.727137	-0.586405	-0.364430
C	17.174860	0.752633	-0.211602
C	16.265557	1.814309	0.039166
C	14.799038	1.562019	0.148819
C	18.555750	1.035614	-0.313365
C	19.463904	-0.025338	-0.568304
C	19.002347	-1.318064	-0.712478
C	17.631643	-1.599433	-0.609707
C	19.000940	2.375967	-0.158933
C	20.446748	2.719279	-0.257877
N	21.283044	1.631338	-0.513276
C	20.875602	0.301883	-0.672402
C	22.671991	1.628868	-0.667158
C	22.998370	0.283979	-0.910522
N	21.858891	-0.513050	-0.906403
C	23.628661	2.636968	-0.618491
C	24.946164	2.246248	-0.826867
C	25.290686	0.907198	-1.072336
C	24.326226	-0.088815	-1.117371
C	16.723452	3.105067	0.184682
C	18.097253	3.386616	0.085768
C	5.130699	1.581498	0.877646
C	6.530967	1.683634	0.817432
O	20.885243	3.843106	-0.132214
O	13.983778	2.433604	0.360892
O	9.362475	1.775512	0.656540

O	2.333045	1.283727	0.962390
N	-2.490384	-3.235119	0.218592
C	-3.253566	-2.174563	0.370417
N	-2.525972	-1.000804	0.578419
C	-3.065914	0.291721	0.764367
C	-4.514613	0.343317	0.712928
C	-5.286392	-0.831631	0.494989
C	-4.685878	-2.102945	0.328617
C	-6.710778	-0.728478	0.434601
C	-7.470879	-1.901843	0.211409
C	-6.843492	-3.149865	0.055704
C	-5.470622	-3.249300	0.113191
C	-7.322569	0.545877	0.593274
C	-6.526022	1.687437	0.815051
C	-5.155471	1.588268	0.873784
C	-8.763522	0.702178	0.524216
N	-9.465445	-0.501646	0.290833
C	-8.897503	-1.768242	0.138575
N	-9.788895	-2.712403	-0.069939
C	-11.005435	-2.064357	-0.064402
C	-10.837555	-0.667119	0.160449
C	-12.273581	-2.607870	-0.251475
C	-13.334694	-1.710741	-0.208226
C	-13.127397	-0.327470	0.017810
C	-11.880818	0.250677	0.211832
N	-14.415637	0.228752	-0.018372
C	-15.291399	-0.837705	-0.261133
N	-14.691038	-1.980754	-0.374781
C	-14.784095	1.555578	0.146228
C	-16.254850	1.810325	0.037886
C	-17.167559	0.752562	-0.212381
C	-16.717346	-0.586272	-0.366337
C	-18.548502	1.036994	-0.312329
C	-19.457133	-0.022943	-0.566714
C	-18.993749	-1.315841	-0.712000
C	-17.624012	-1.598728	-0.611297
C	-18.990687	2.378405	-0.156300
C	-18.082517	3.386209	0.088055
C	-16.709590	3.101937	0.185039
C	-20.433080	2.723192	-0.253170
N	-21.272184	1.635125	-0.508410
C	-20.867832	0.304530	-0.668892
N	-21.855128	-0.507827	-0.901992
C	-22.991401	0.292846	-0.903672
C	-22.660778	1.636925	-0.659996
C	-24.321104	-0.074487	-1.108493
C	-25.283025	0.924346	-1.061384
C	-24.934308	2.262006	-0.815709
C	-23.614733	2.647515	-0.609276
O	-2.316055	1.245183	0.943812
O	-9.380541	1.754706	0.645341
O	-13.977974	2.436795	0.358854
O	-20.875596	3.846526	-0.127147
H	-19.708494	-2.108595	-0.906469
H	-17.255694	-2.612425	-0.726471
H	-18.448369	4.400946	0.203855
H	-15.987679	3.888781	0.375356
H	-23.335224	3.675350	-0.419612
H	-25.713707	3.017150	-0.786208
H	-26.327053	0.670362	-1.218011
H	-24.577297	-1.111512	-1.297154
H	-7.464999	-4.022687	-0.114081
H	-4.969179	-4.203316	-0.010289
H	-7.026564	2.642331	0.934268
H	-4.535049	2.462197	1.040950
H	-11.722191	1.304559	0.382415
H	-12.423549	-3.666618	-0.425921
H	4.948356	-4.163902	0.005984
H	7.448870	-3.988384	-0.097395
H	4.513115	2.457630	1.042816
H	7.022665	2.643399	0.935322
H	-0.054019	0.472575	0.843145
H	0.005081	-4.546741	0.029935
H	17.263886	-2.613525	-0.723976
H	19.716652	-2.110874	-0.907290
H	16.005467	3.895451	0.375359
H	18.465777	4.400399	0.200307
H	11.757854	1.326561	0.386933
H	12.415144	-3.653110	-0.413550
H	24.578867	-1.126630	-1.305773
H	26.333622	0.650463	-1.230325
H	25.728083	2.998643	-0.799167
H	23.354243	3.666201	-0.429135

E = -4772.02121893 Hartree

BBL, n = 8, ωB97X-D/6-31G*, neutral state

C	0.006655	-3.509140	-0.366903
C	1.163215	-4.274713	-0.302592
C	1.183644	-5.674786	-0.080179
C	0.009520	-6.396550	0.096772
C	-1.165915	-5.657526	0.042105
C	-1.148141	-4.258300	-0.185303
N	2.510025	-3.922550	-0.417708
C	3.238636	-5.107895	-0.260063
N	2.491240	-6.148989	-0.063534
C	4.690241	-5.062464	-0.317327
C	5.305000	-3.798867	-0.521028
C	4.537336	-2.613923	-0.676717
C	3.048754	-2.652490	-0.628432
C	5.157908	-1.399785	-0.870804
C	6.560822	-1.317504	-0.914110
C	7.329236	-2.450780	-0.763410
C	6.714994	-3.716207	-0.565587
C	7.483474	-4.899509	-0.406339
C	8.930902	-4.776188	-0.441481
N	9.506734	-3.514658	-0.634371
C	8.812742	-2.316087	-0.806653
N	9.803845	-5.724412	-0.300356
C	11.044285	-5.102387	-0.393591
C	10.889886	-3.709045	-0.604471
C	11.944708	-2.814565	-0.729539
C	13.187083	-3.425445	-0.621537
C	13.378584	-4.814098	-0.409299
C	12.301827	-5.684447	-0.292992
N	14.481289	-2.901577	-0.674574
C	15.348358	-3.985368	-0.491071
N	14.734026	-5.116453	-0.335700
C	16.782778	-3.755307	-0.481940
C	17.240623	-2.423999	-0.665555
C	16.335725	-1.345973	-0.857561
C	14.862616	-1.572449	-0.866178

C	16.806930	-0.063737	-1.034640
C	18.189239	0.193856	-1.024499
C	19.088142	-0.832633	-0.835619
C	18.629604	-2.164686	-0.652864
C	19.533569	-3.240984	-0.453898
C	20.953976	-2.937238	-0.431578
N	21.375832	-1.614568	-0.613120
C	20.544171	-0.513059	-0.822501
C	22.770661	-1.636390	-0.528807
C	23.087113	-2.999281	-0.298983
N	21.930615	-3.769658	-0.248069
C	23.712952	-0.620786	-0.624823
C	25.016034	-1.074848	-0.467562
C	25.367894	-2.428435	-0.235526
C	24.401646	-3.422691	-0.148289
N	26.746638	-2.562510	-0.112545
C	27.223926	-1.365753	-0.257261
N	26.237606	-0.397124	-0.480152
C	26.458983	0.968078	-0.667291
C	27.891284	1.374777	-0.606059
C	28.914463	0.416803	-0.375511
C	28.618472	-0.960870	-0.201020
C	30.259195	0.846608	-0.312084
C	31.282327	-0.109194	-0.075353
C	30.967626	-1.443175	0.086112
C	29.632157	-1.870146	0.022917
C	30.553474	2.225716	-0.482300
C	29.542818	3.133288	-0.709948
C	28.204848	2.705753	-0.771741
C	31.955076	2.725733	-0.410531
N	32.909028	1.737308	-0.165396
C	32.651984	0.371113	0.002700
N	33.719412	-0.328805	0.230516
C	34.768861	0.584198	0.227908
C	34.289270	1.895090	-0.019269
C	36.119289	0.336020	0.441121
C	36.950031	1.448955	0.398698
C	36.435404	2.745877	0.147029
C	35.093385	3.025973	-0.073046
N	38.326870	1.496407	0.589763
C	38.649249	2.746046	0.466074
N	37.556855	3.577977	0.191915
C	37.607707	4.960615	0.007341
C	38.969605	5.551014	0.137673
C	40.096510	4.734527	0.422678
C	39.973860	3.330081	0.590009
C	41.369942	5.335037	0.543921
C	42.496906	4.519524	0.829165
C	42.349840	3.156441	0.986545
C	41.085313	2.560199	0.866940
C	41.491845	6.740683	0.378601
C	40.382955	7.509066	0.100039
C	39.116096	6.911412	-0.021565
C	42.815095	7.415612	0.503998
N	43.877461	6.556945	0.785019
C	43.790927	5.169707	0.947594
N	44.934604	4.608591	1.195971
C	45.856293	5.650195	1.206644
C	45.226584	6.880416	0.954034
C	47.232729	5.598290	1.425027
C	47.936727	6.792741	1.383050
C	47.290022	8.013395	1.130314
C	45.919712	8.085095	0.909678
C	17.683295	-4.784144	-0.294706
C	19.062156	-4.526325	-0.279876
C	5.460708	-6.198057	-0.170242
C	6.860965	-6.116164	-0.215130
O	25.545895	1.741719	-0.858895
O	32.262993	3.890100	-0.546443
O	36.612228	5.608162	-0.235162
O	42.976398	8.610479	0.375926
O	20.991068	0.603093	-0.974928
O	14.045594	-0.690963	-1.021878
O	9.389561	-1.263102	-0.972248
O	2.344613	-1.674230	-0.755486
N	-2.471566	-6.112541	0.194256
C	-3.220130	-5.061189	0.069903
C	-4.669426	-4.995392	0.156404
C	-5.284942	-3.726338	-0.007132
C	-4.520823	-2.554258	-0.252061
C	-3.034867	-2.612347	-0.342156
N	-2.494591	-3.887071	-0.166242
C	-5.436419	-6.117992	0.393792
C	-6.833773	-6.018192	0.476578
C	-7.456856	-4.796646	0.321698
C	-6.692004	-3.625770	0.076303
C	-7.306747	-2.355624	-0.086635
C	-8.786669	-2.203055	-0.003707
N	-9.477169	-3.391460	0.238719
C	-8.901078	-4.657273	0.400829
C	-10.856808	-3.572585	0.362868
C	-11.009188	-4.962826	0.594423
N	-9.770832	-5.595689	0.610588
C	-12.263403	-5.534416	0.769169
C	-13.338926	-4.657459	0.700967
C	-13.149427	-3.271752	0.468404
C	-11.910283	-2.670799	0.290527
N	-14.691611	-4.951579	0.834536
C	-15.306290	-3.818908	0.692691
N	-14.441908	-2.741013	0.466631
C	-16.739222	-3.584011	0.739925
C	-17.198441	-2.254311	0.548206
C	-16.295864	-1.180838	0.322662
C	-14.824283	-1.412123	0.275431
C	-17.637649	-4.608708	0.957465
C	-19.015984	-4.349303	0.988866
C	-19.488969	-3.066246	0.802676
C	-18.586752	-1.993008	0.580184
C	-19.046577	-0.663045	0.385998
C	-20.502341	-0.343247	0.406145
N	-21.332786	-1.443693	0.625184
C	-20.909901	-2.764193	0.819559
C	-22.728704	-1.469820	0.684411
C	-23.044984	-2.832522	0.915524
N	-21.886862	-3.598355	0.993486
C	-24.361496	-3.261929	1.027543
C	-25.329784	-2.274321	0.897038
C	-24.977600	-0.920149	0.668880
C	-23.672486	-0.459608	0.553528
N	-26.202142	-0.252142	0.592994
C	-27.190854	-1.227270	0.772795
N	-26.711910	-2.418325	0.954598
C	-16.768189	0.100090	0.139223
C	-18.149675	0.360040	0.171092

C	-5.142122	-1.335065	-0.408591
C	-6.542049	-1.235011	-0.325269
C	-26.424378	1.109622	0.383473
C	-27.861484	1.501765	0.348538
C	-28.888003	0.534476	0.516730
C	-28.590214	-0.836959	0.732408
C	-30.238596	0.947260	0.465446
C	-30.534561	2.319759	0.251041
C	-29.520024	3.238104	0.095347
C	-28.176443	2.826845	0.143166
C	-31.266041	-0.019889	0.625433
C	-30.949028	-1.346695	0.834636
C	-29.607585	-1.756061	0.889491
C	-31.943408	2.799505	0.186175
N	-32.902395	1.798416	0.344573
C	-32.643771	0.438076	0.553010
N	-33.718780	-0.279996	0.654021
C	-34.775880	0.612443	0.507487
C	-34.292441	1.930685	0.312721
C	-35.102899	3.043690	0.132473
C	-36.456535	2.735962	0.156198
C	-36.975963	1.430040	0.343331
C	-36.137783	0.337050	0.526649
N	-37.588654	3.540650	0.006789
C	-38.692177	2.684432	0.106075
N	-38.366274	1.445389	0.304998
C	-40.031015	3.233698	-0.024874
C	-40.155230	4.631141	-0.242950
C	-39.015835	5.475133	-0.328551
C	-37.639134	4.920122	-0.199648
C	-41.443073	5.196336	-0.380040
C	-41.566870	6.594701	-0.597409
C	-40.445372	7.391131	-0.672268
C	-39.163920	6.828547	-0.537691
C	-42.582618	4.352869	-0.299405
C	-42.433776	2.997638	-0.086195
C	-41.155081	2.436606	0.052117
C	-42.905756	7.231624	-0.752310
N	-43.979978	6.346313	-0.666596
C	-43.891024	4.966274	-0.452112
N	-45.046163	4.375778	-0.416877
C	-45.978906	5.388171	-0.616143
C	-45.344042	6.631405	-0.775470
C	-46.046526	7.812016	-0.991409
C	-47.430998	7.702006	-1.044074
C	-48.082490	6.467948	-0.887214
C	-47.369437	5.297802	-0.671581
O	-20.950308	0.771417	0.246054
O	-14.009476	-0.535103	0.086490
O	-9.363590	-1.145056	-0.133152
O	-2.333693	-1.645479	-0.548321
O	-25.508711	1.890974	0.242006
O	-32.253294	3.957697	0.008383
O	-36.632182	5.591382	-0.267457
O	-43.069136	8.418405	-0.939209
H	-43.320395	2.375218	-0.029317
H	-41.032582	1.371782	0.218621
H	-40.570331	8.455671	-0.838218
H	-38.275875	7.448588	-0.597679
H	-45.536658	8.758614	-1.111843
H	-48.022583	8.596568	-1.211674
H	-49.166301	6.431742	-0.937534
H	-47.861042	4.338939	-0.548884
H	-31.751577	-2.066856	0.952817
H	-29.354571	-2.798094	1.052860
H	-29.776165	4.279467	-0.066988
H	-27.371955	3.543606	0.018380
H	-34.720137	4.042338	-0.014122
H	-36.522289	-0.665363	0.670544
H	-19.726891	-5.151188	1.156844
H	-17.260181	-5.615448	1.101152
H	-18.529261	1.365753	0.025877
H	-16.056134	0.900518	-0.030813
H	-23.419431	0.574953	0.377311
H	-24.615408	-4.300510	1.201105
H	-7.440587	-6.897606	0.663769
H	-4.942253	-7.075774	0.516404
H	-7.038431	-0.278300	-0.446657
H	-4.532907	-0.457384	-0.595748
H	-11.778301	-1.614076	0.113866
H	-12.395079	-6.594958	0.945473
H	4.967239	-7.151610	-0.015938
H	7.470580	-7.005431	-0.096119
H	4.546145	-0.511602	-0.986390
H	7.056397	-0.364348	-1.063489
H	0.005241	-2.443061	-0.536594
H	0.010737	-7.465734	0.270741
H	17.306780	-5.791919	-0.155843
H	19.774478	-5.330363	-0.129050
H	16.093045	0.740145	-1.178835
H	18.567616	1.201100	-1.162095
H	11.811948	-1.755249	-0.889298
H	12.434820	-6.746715	-0.128508
H	29.380311	-2.916956	0.154423
H	31.766971	-2.153871	0.266712
H	27.403458	3.415444	-0.946524
H	29.797189	4.179926	-0.837434
H	23.460387	0.414147	-0.799645
H	24.655171	-4.460515	0.030288
H	40.963778	1.489704	0.992674
H	43.226773	2.556496	1.205158
H	38.237871	7.509409	-0.240250
H	40.506137	8.579598	-0.022951
H	34.713769	4.019021	-0.260417
H	36.499908	-0.659642	0.633683
H	47.720982	4.649440	1.618512
H	49.009543	6.787162	1.548876
H	47.874448	8.927897	1.106194
H	45.412545	9.020701	0.714397

E = -9311.69545819 Hartree

BBL, n = 8, (U)ωB97X-D/6-31G*, charged (-1) state

C	0.006309	-3.539721	-0.369450
C	1.164534	-4.303295	-0.304178
C	1.184958	-5.704421	-0.081142
C	0.009207	-6.424838	0.094602
C	-1.167858	-5.687506	0.038987
C	-1.150122	-4.287220	-0.188954
N	2.511138	-3.951172	-0.417626
C	3.239671	-5.135732	-0.258728
N	2.489989	-6.179816	-0.062438

C	4.687528	-5.089119	-0.313987
C	5.299643	-3.825469	-0.517795
C	4.529230	-2.641642	-0.675241
C	3.050263	-2.679468	-0.629233
C	5.156128	-1.422624	-0.870255
C	6.551478	-1.339579	-0.911481
C	7.328607	-2.475676	-0.758545
C	6.713169	-3.741552	-0.560644
C	7.479829	-4.924249	-0.399437
C	8.923442	-4.800861	-0.432896
N	9.497606	-3.539041	-0.625499
C	8.801423	-2.339192	-0.799728
N	9.800376	-5.750499	-0.290829
C	11.036836	-5.125289	-0.383488
C	10.880227	-3.730808	-0.594791
C	11.935583	-2.836128	-0.719082
C	13.180076	-3.443160	-0.610950
C	13.373661	-4.832583	-0.398455
C	12.296336	-5.703611	-0.282649
N	14.473882	-2.917569	-0.663591
C	15.341915	-4.000002	-0.479960
N	14.726746	-5.134987	-0.324364
C	16.771645	-3.769580	-0.470872
C	17.226998	-2.438315	-0.654591
C	16.318818	-1.362385	-0.846209
C	14.854268	-1.587759	-0.855006
C	16.793511	-0.073227	-1.024138
C	18.167456	0.184600	-1.014387
C	19.076702	-0.843722	-0.825203
C	18.619795	-2.176936	-0.642298
C	19.521435	-3.253831	-0.443648
C	20.936866	-2.952869	-0.421725
N	21.355855	-1.630296	-0.603468
C	20.520072	-0.524273	-0.812843
C	22.747952	-1.647154	-0.521152
C	23.069711	-3.011149	-0.291400
N	21.920583	-3.785510	-0.238906
C	23.687144	-0.628008	-0.618766
C	24.992750	-1.075109	-0.463753
C	25.349482	-2.426796	-0.231930
C	24.387914	-3.425686	-0.142977
N	26.729968	-2.555424	-0.110534
C	27.203333	-1.357820	-0.255997
N	26.214091	-0.391551	-0.478098
C	26.433995	0.970353	-0.666150
C	27.868388	1.379858	-0.605685
C	28.893961	0.424950	-0.375367
C	28.597790	-0.952836	-0.200330
C	30.238236	0.856491	-0.312694
C	31.261832	-0.098295	-0.076054
C	30.947261	-1.432545	0.086004
C	29.612532	-1.861195	0.023507
C	30.529798	2.236255	-0.483711
C	29.516200	3.141183	-0.711265
C	28.179055	2.711189	-0.772233
C	31.928818	2.737672	-0.412788
N	32.885284	1.749480	-0.167058
C	32.630754	0.382759	0.001571
N	33.700456	-0.315049	0.229137
C	34.747216	0.600379	0.225771
C	34.264515	1.910486	-0.021674
C	36.098247	0.356041	0.438476
C	36.926553	1.471069	0.395473
C	36.409202	2.766391	0.143623
C	35.066408	3.043055	-0.076053
N	38.303702	1.521750	0.586322
C	38.623439	2.771815	0.462289
N	37.529418	3.601579	0.188039
C	37.578323	4.983159	0.003209
C	38.940181	5.576140	0.133334
C	40.068611	4.762029	0.418473
C	39.947426	3.357419	0.586205
C	41.341173	5.364484	0.539377
C	42.469130	4.550651	0.824931
C	42.323548	3.187399	0.982820
C	41.059948	2.589199	0.863441
C	41.460551	6.770327	0.373317
C	40.349989	7.536439	0.094622
C	39.084096	6.936638	-0.026469
C	42.782151	7.447028	0.497970
N	43.846209	6.589870	0.779598
C	43.762207	5.202578	0.943115
N	44.907236	4.643853	1.191966
C	45.826631	5.687370	1.201946
C	45.194461	6.916167	0.948390
C	47.203158	5.638820	1.420507
C	47.904783	6.834731	1.377742
C	47.255649	8.053819	1.124007
C	45.885169	8.122218	0.903198
C	17.676213	-4.803004	-0.282909
C	19.048189	-4.545218	-0.268571
C	5.461258	-6.228594	-0.164282
C	6.855731	-6.145963	-0.207239
O	25.525139	1.749098	-0.858756
O	32.239297	3.901771	-0.549054
O	36.583349	5.631371	-0.239582
O	42.943150	8.642051	0.369238
O	20.981797	0.590361	-0.964095
O	14.030612	-0.706385	-1.011068
O	9.387463	-1.286063	-0.965418
O	2.337569	-1.702210	-0.757940
N	-2.470917	-6.144135	0.190409
C	-3.221768	-5.090007	0.065153
C	-4.667310	-5.023518	0.150694
C	-5.280262	-3.754480	-0.013228
C	-4.513471	-2.583204	-0.258006
C	-3.037074	-2.640038	-0.347122
N	-2.496361	-3.916432	-0.170793
C	-5.437443	-6.150269	0.388904
C	-6.829035	-6.050181	0.470957
C	-7.453783	-4.823628	0.315187
C	-6.690807	-3.653004	0.070012
C	-7.306806	-2.382453	-0.093089
C	-8.776120	-2.228657	-0.011450
N	-9.468670	-3.418539	0.231651
C	-8.894202	-4.684528	0.394113
C	-10.847750	-3.597180	0.355722
C	-11.002289	-4.988521	0.587921
N	-9.767878	-5.624370	0.604731
C	-12.258428	-5.556421	0.762651
C	-13.334520	-4.678842	0.694560
C	-13.142957	-3.292405	0.461515
C	-11.901737	-2.695272	0.283575
N	-14.684824	-4.973039	0.828471
C	-15.300353	-3.836504	0.686146
N	-14.435024	-2.759990	0.459847
C	-16.728556	-3.601183	0.733602
C	-17.185252	-2.271463	0.542161
C	-16.279420	-1.200143	0.316569
C	-14.816434	-1.430385	0.268918
C	-17.631009	-4.630405	0.952309
C	-19.002409	-4.370911	0.983969
C	-19.477193	-3.081692	0.797393
C	-18.577339	-2.007958	0.574637
C	-19.035557	-0.676817	0.380486
C	-20.478651	-0.357032	0.400506
N	-21.313190	-1.461847	0.620621
C	-20.893068	-2.782216	0.815288
C	-22.706291	-1.482807	0.679984
C	-23.027680	-2.846462	0.912325
N	-21.876926	-3.616340	0.990730
C	-24.347663	-3.266952	1.024367

C	-25.311446	-2.274761	0.893374
C	-24.954561	-0.922642	0.664469
C	-23.647181	-0.469103	0.548744
N	-26.178810	-0.248685	0.588287
C	-27.170319	-1.221202	0.769004
N	-26.695244	-2.413141	0.951175
C	-16.755246	0.087768	0.132689
C	-18.128349	0.348015	0.164610
C	-5.141128	-1.359147	-0.415201
C	-6.533538	-1.258842	-0.332830
C	-26.399330	1.109936	0.379016
C	-27.838422	1.505191	0.344553
C	-28.867374	0.541149	0.513526
C	-28.569523	-0.830484	0.729437
C	-30.217441	0.955967	0.462967
C	-30.510534	2.329205	0.248171
C	-29.493026	3.244688	0.091510
C	-28.150353	2.830700	0.138746
C	-31.245432	-0.009913	0.624041
C	-30.928657	-1.337065	0.833366
C	-29.588015	-1.748404	0.887527
C	-31.916681	2.810720	0.184231
N	-32.878258	1.810085	0.344038
C	-32.622379	0.449131	0.552629
N	-33.699799	-0.266436	0.654642
C	-34.754045	0.628808	0.508551
C	-34.267236	1.946105	0.313108
C	-35.075117	3.061215	0.133278
C	-36.429618	2.757400	0.157913
C	-36.952064	1.453213	0.345493
C	-36.116621	0.357777	0.528512
N	-37.560391	3.565518	0.008949
C	-38.665741	2.711761	0.108984
N	-38.342728	1.472185	0.307888
C	-40.003916	3.262875	-0.021305
C	-40.126444	4.660526	-0.239533
C	-38.985319	5.501930	-0.325744
C	-37.608670	4.944008	-0.197265
C	-41.413402	5.227923	-0.376045
C	-41.534499	6.626588	-0.593525
C	-40.411143	7.420528	-0.669023
C	-39.130683	6.855516	-0.534999
C	-42.554104	4.386292	-0.294706
C	-42.406962	3.030824	-0.081398
C	-41.129217	2.467605	0.056370
C	-42.871714	7.265564	-0.747691
N	-43.947826	6.381829	-0.661387
C	-43.861553	5.001635	-0.446813
N	-45.018200	4.413582	-0.410998
C	-45.948611	5.428046	-0.609949
C	-45.311100	6.669906	-0.769652
C	-46.011098	7.852059	-0.985294
C	-47.395897	7.745438	-1.037335
C	-48.050006	6.512869	-0.880127
C	-47.339376	5.341112	-0.664785
O	-20.941367	0.756151	0.241718
O	-13.994968	-0.553530	0.079471
O	-9.362333	-1.170542	-0.140730
O	-2.327463	-1.673917	-0.553513
O	-25.487713	1.896127	0.236047
O	-32.229059	3.968688	0.006346
O	-36.602027	5.615656	-0.265825
O	-43.034670	8.452593	-0.934583
H	-43.294519	2.409740	-0.024005
H	-41.007986	1.402658	0.222904
H	-40.533943	8.485326	-0.835080
H	-38.241187	7.473414	-0.595499
H	-45.498633	8.797255	-1.105898
H	-47.985439	8.641442	-1.204681
H	-49.133976	6.479008	-0.929901
H	-47.833036	4.383304	-0.541836
H	-31.731809	-2.056558	0.952335
H	-29.335183	-2.790419	1.050949
H	-29.746441	4.286714	-0.071226
H	-27.343648	3.544783	0.013240
H	-34.688893	4.058473	-0.013654
H	-36.503787	-0.643581	0.672722
H	-19.715894	-5.170588	1.151965
H	-17.250576	-5.636034	1.095378
H	-18.507540	1.353945	0.019692
H	-16.039654	0.884944	-0.037055
H	-23.385320	0.562956	0.371679
H	-24.607021	-4.304190	1.198418
H	-7.438881	-6.927539	0.658093
H	-4.940810	-7.106784	0.511398
H	-7.031150	-0.302799	-0.454302
H	-4.529437	-0.483186	-0.602187
H	-11.767143	-1.638972	0.106567
H	-12.391665	-6.616906	0.939262
H	4.965344	-7.180883	-0.010013
H	7.468491	-7.032949	-0.087085
H	4.541802	-0.536398	-0.987050
H	7.048241	-0.387041	-1.060768
H	0.004842	-2.473793	-0.539250
H	0.010456	-7.494133	0.269084
H	17.296715	-5.809611	-0.144287
H	19.763107	-5.347128	-0.118220
H	16.076072	0.727405	-1.167934
H	18.545448	1.192026	-1.151912
H	11.800252	-1.777171	-0.878792
H	12.430901	-6.765836	-0.117929
H	29.360739	-2.907907	0.155463
H	31.747166	-2.142718	0.266705
H	27.375377	3.418286	-0.946869
H	29.767918	4.188443	-0.839390
H	23.424917	0.404391	-0.793525
H	24.647210	-4.462174	0.035562
H	40.939560	1.518633	0.989539
H	43.201245	2.588633	1.201742
H	38.204534	7.532656	-0.245151
H	40.471188	8.607158	-0.028889
H	34.683667	4.034780	-0.263723
H	36.481212	-0.638689	0.631279
H	47.693327	4.691089	1.614799
H	48.977637	6.831429	1.543762
H	47.838065	8.969629	1.099254
H	45.375662	9.056408	0.707149

E = -9311.77140629 Hartree

BBL, n = 8, (U)ωB97X-D/6-31G* broken symmetry (BS), charged (-1) state

C	0.027004	-3.591898	0.356401
C	1.178675	-4.348841	0.172353
C	1.189965	-5.755870	-0.056589
C	0.000301	-6.477187	-0.107012
C	-1.167177	-5.743749	0.072546
C	-1.137228	-4.344534	0.295224
N	2.518079	-3.985961	0.151881
C	3.242272	-5.156405	-0.084600
N	2.478629	-6.219945	-0.209664
C	4.672431	-5.080869	-0.168634
C	5.275289	-3.810588	-0.003445
C	4.507363	-2.638625	0.242122
C	3.060248	-2.693198	0.329503
C	5.150864	-1.395023	0.402580
C	6.520332	-1.295076	0.321825

C	7.313301	-2.434463	0.076797
C	6.698368	-3.706606	-0.087487
C	7.454305	-4.878027	-0.333362
C	8.880427	-4.746577	-0.412733
N	9.452434	-3.483196	-0.248887
C	8.753878	-2.279624	-0.002412
N	9.768918	-5.692302	-0.626692
C	10.987730	-5.049784	-0.606758
C	10.824641	-3.653364	-0.371209
C	11.872534	-2.742337	-0.295580
C	13.118834	-3.326814	-0.472468
C	13.320742	-4.709586	-0.707482
C	12.254977	-5.599227	-0.779762
N	14.412549	-2.781576	-0.467549
C	15.285152	-3.853836	-0.694804
N	14.678240	-4.989888	-0.839337
C	16.716416	-3.618943	-0.741496
C	17.176538	-2.288554	-0.548694
C	16.267030	-1.222610	-0.322836
C	14.789541	-1.460689	-0.276353
C	16.731702	0.060575	-0.137656
C	18.111350	0.327464	-0.168512
C	19.016783	-0.689607	-0.384083
C	18.564134	-2.022211	-0.579997
C	19.468367	-3.092417	-0.803293
C	20.886853	-2.787853	-0.820011
N	21.303270	-1.464986	-0.623949
C	20.466280	-0.364850	-0.403508
C	22.697650	-1.481954	-0.682628
C	23.022298	-2.843522	-0.915570
N	21.870786	-3.616656	-0.995010
C	23.635899	-0.466401	-0.550338
C	24.944335	-0.917764	-0.665932
C	25.304082	-2.268733	-0.895523
C	24.341653	-3.262652	-1.027496
N	26.687752	-2.404550	-0.952977
C	27.160288	-1.211624	-0.769869
N	26.166632	-0.241581	-0.588922
C	26.383713	1.118255	-0.378610
C	27.821510	1.516818	-0.343433
C	28.852570	0.555011	-0.512682
C	28.558445	-0.817245	-0.729520
C	30.201597	0.973039	-0.461410
C	31.232006	0.009704	-0.622687
C	30.918783	-1.318067	-0.832889
C	29.579113	-1.732618	-0.887769
C	30.491491	2.346787	-0.245718
C	29.472073	3.259964	-0.088796
C	28.130298	2.842902	-0.136707
C	31.896859	2.831635	-0.181047
N	32.860678	1.833486	-0.341272
C	32.607868	0.472080	-0.550548
N	33.686717	-0.241101	-0.652608
C	34.739072	0.656299	-0.505837
C	34.249453	1.972447	-0.309932
C	36.102166	0.387956	-0.525606
C	36.935252	1.485010	-0.341919
C	36.410101	2.788100	-0.153934
C	35.054966	3.089173	-0.129468
N	38.325811	1.506721	-0.304016
C	38.646246	2.746873	-0.104561
N	37.539186	3.598375	-0.004431
C	37.584733	4.977020	0.202181
C	38.960253	5.537581	0.331022
C	40.103018	4.698372	0.244770
C	39.983274	3.300558	0.026177
C	41.388885	5.268152	0.381585
C	42.531181	4.428674	0.300232
C	42.386706	3.072972	0.086607
C	41.110058	2.507403	-0.051508
C	41.507334	6.666999	0.599366
C	40.382467	7.458788	0.674894
C	39.103066	6.891405	0.540595
C	42.843385	7.308425	0.753810
N	43.921147	6.426702	0.667544
C	43.837445	5.046410	0.452676
N	44.995159	4.460478	0.416919
C	45.923678	5.476598	0.616225
C	45.283878	6.717257	0.776078
C	47.314591	5.392168	0.671263
C	48.023037	6.565176	0.886932
C	47.366655	7.796527	1.044267
C	45.981667	7.900650	0.992043
C	17.619190	-4.641233	-0.959938
C	18.995380	-4.376730	-0.990391
C	5.452825	-6.224593	-0.411650
C	6.824343	-6.124310	-0.492853
O	25.469286	1.900859	-0.235714
O	32.205923	3.990255	-0.002320
O	36.576664	5.646495	0.270675
O	43.004099	8.495707	0.940953
O	20.919990	0.748844	-0.243331
O	13.986638	-0.571802	-0.085553
O	9.374036	-1.229567	0.123970
O	2.313747	-1.742467	0.534965
N	-2.480184	-6.207867	0.058220
C	-3.222515	-5.163872	0.256067
C	-4.672530	-5.121433	0.313321
C	-5.291030	-3.858684	0.518551
C	-4.518263	-2.678393	0.673970
C	-3.022892	-2.719615	0.624656
N	-2.487729	-3.981162	0.413032
C	-5.445145	-6.256979	0.165814
C	-6.844100	-6.173028	0.211544
C	-7.469566	-4.956675	0.404375
C	-6.701134	-3.774343	0.564103
C	-7.311276	-2.506782	0.763448
C	-8.789220	-2.369545	0.807950
N	-9.487194	-3.569991	0.634397
C	-8.915254	-4.833613	0.440034
C	-10.869414	-3.757474	0.606032
C	-11.030263	-5.150999	0.394390
N	-9.794357	-5.779056	0.299422
C	-12.291285	-5.724961	0.295387
C	-13.363998	-4.848790	0.413660
C	-13.165985	-3.462088	0.626262
C	-11.920115	-2.858054	0.732890
N	-14.721779	-5.144555	0.341348
C	-15.331049	-4.011340	0.497773
N	-14.459317	-2.931143	0.680965
C	-16.764935	-3.778027	0.489358
C	-17.219960	-2.445524	0.673431
C	-16.310533	-1.371704	0.865085
C	-14.835960	-1.603581	0.873170

C	-17.668693	-4.804177	0.302338
C	-19.046537	-4.541748	0.288215
C	-19.514936	-3.255120	0.462639
C	-18.608123	-2.181589	0.661371
C	-19.061365	-0.847584	0.844519
C	-20.514671	-0.523429	0.832037
N	-21.350932	-1.623305	0.622741
C	-20.934123	-2.947592	0.440647
C	-22.745226	-1.639054	0.538900
C	-23.067391	-3.000903	0.308605
N	-21.914743	-3.776226	0.257184
C	-24.383691	-3.418001	0.157886
C	-25.345771	-2.419484	0.245482
C	-24.988640	-1.067740	0.478131
C	-23.683472	-0.619607	0.635485
N	-26.208155	-0.384651	0.490600
C	-27.197928	-1.349565	0.266751
N	-26.725283	-2.547891	0.121862
C	-16.776226	-0.087764	1.042506
C	-18.157529	0.175064	1.032967
C	-5.134346	-1.462424	0.869365
C	-6.536399	-1.376420	0.913867
C	-26.425415	0.980099	0.678584
C	-27.857280	1.391829	0.616000
C	-28.883632	0.437827	0.383866
C	-28.591271	-0.940660	0.209174
C	-30.226874	0.872076	0.318924
C	-30.516583	2.252200	0.489371
C	-29.502691	3.155926	0.718727
C	-28.166260	2.723715	0.782004
C	-31.252413	-0.080489	0.080469
C	-30.941350	-1.415370	-0.081167
C	-29.607441	-1.846753	-0.016436
C	-31.915771	2.756622	0.415877
N	-32.873054	1.770892	0.168727
C	-32.620372	0.403870	0.000644
N	-33.690131	-0.292446	-0.228678
C	-34.736124	0.624225	-0.227162
C	-34.252262	1.933544	0.020965
C	-35.052768	3.067079	0.074029
C	-36.395489	2.791719	-0.147746
C	-36.914109	1.496795	-0.400400
C	-36.087086	0.380955	-0.442060
N	-37.514331	3.627873	-0.193695
C	-38.609042	2.799581	-0.469505
N	-38.290711	1.549015	-0.593187
C	-39.931885	3.387379	-0.594864
C	-40.050937	4.792066	-0.426714
C	-38.921827	5.604791	-0.139954
C	-37.561378	5.010112	-0.008554
C	-41.322517	5.396302	-0.548799
C	-41.440323	6.802187	-0.382249
C	-40.329274	7.566913	-0.101987
C	-39.064267	6.965459	0.020227
C	-42.451390	4.584204	-0.836006
C	-42.307818	3.220819	-0.994318
C	-41.045166	2.620845	-0.873688
C	-42.761196	7.480833	-0.507996
N	-43.825892	6.625380	-0.791297
C	-43.743437	5.238082	-0.955350
N	-44.888718	4.680842	-1.205773
C	-45.806967	5.725428	-1.216356
C	-45.173643	6.953332	-0.961477
C	-45.862895	8.160207	-0.916486
C	-47.233167	8.093414	-1.138939
C	-47.883482	6.875201	-1.394034
C	-47.183298	5.678481	-1.436571
O	-20.961526	0.593116	0.984481
O	-14.020783	-0.720474	1.029773
O	-9.373776	-1.319588	0.974967
O	-2.334064	-1.729861	0.755653
O	-25.511863	1.752656	0.872047
O	-32.221761	3.921613	0.551835
O	-36.564971	5.655621	0.235408
O	-42.920088	8.675968	-0.378649
H	-43.186158	2.623470	-1.214458
H	-40.926309	1.550127	-1.000025
H	-40.449369	8.637708	0.021863
H	-38.184336	7.560491	0.240134
H	-45.352643	9.093772	-0.719390
H	-47.814568	9.009853	-1.114425
H	-48.956125	6.873337	-1.561267
H	-47.674363	4.731438	-1.631887
H	-31.742603	-2.123571	-0.263263
H	-29.358365	-2.894174	-0.148153
H	-29.753222	4.203486	0.846379
H	-27.362370	3.430246	0.958067
H	-34.669806	4.058643	0.262207
H	-36.470825	-0.613372	-0.635332
H	-19.761140	-5.343863	0.137430
H	-17.294618	-5.812752	0.163051
H	-18.531366	1.184012	1.170778
H	-16.058312	0.712581	1.186291
H	-23.424947	0.413732	0.810786
H	-24.641671	-4.454647	-0.021225
H	-7.453628	-7.062565	0.091810
H	-4.950390	-7.209534	0.010456
H	-7.028553	-0.421431	1.064169
H	-4.516819	-0.578268	0.984427
H	-11.778900	-1.799865	0.892883
H	-12.429976	-6.786451	0.130303
H	4.949306	-7.177716	-0.533473
H	7.442951	-6.995494	-0.680659
H	4.533597	-0.523079	0.590560
H	7.022720	-0.341506	0.443830
H	0.052453	-2.525984	0.525274
H	-0.014679	-7.546610	-0.280801
H	17.242602	-5.648034	-1.104423
H	19.708195	-5.177143	-1.158970
H	16.012369	0.854359	0.032610
H	18.484483	1.335549	-0.021850
H	11.717424	-1.689411	-0.115835
H	12.401696	-6.657735	-0.958257
H	29.329047	-2.775195	-1.051890
H	31.723714	-2.035523	-0.951976
H	27.322112	3.555286	-0.010984
H	29.723047	4.302454	0.074649
H	23.373319	0.565404	-0.372685
H	24.602301	-4.299432	-1.202118
H	40.990828	1.442271	-0.218316
H	43.275481	2.453637	0.029215
H	38.212424	7.507645	0.601135
H	40.503255	8.523782	0.841182
H	34.666785	4.085643	0.017760

H	36.491401	-0.612543	-0.670148
H	47.809971	4.435262	0.548216
H	49.107060	6.533315	0.936864
H	47.954530	8.693583	1.211835
H	45.467432	8.844886	1.112711

E = -9311.78699501 Hartree

P(NDI2OD-T2), n = 5, ωB97X-D/6-31G*, neutral state

C	25.711878	-0.331342	-0.278476
C	24.726486	-1.324386	-0.459311
C	23.440044	-0.975854	-0.774452
C	23.051409	0.370635	-0.958955
C	24.012721	1.363133	-0.828222
C	25.338667	1.017301	-0.465832
C	26.320261	2.012954	-0.274499
C	27.584427	1.670930	0.121632
C	27.967634	0.325288	0.333830
C	27.037613	-0.677160	0.091199
C	23.704038	2.792964	-1.134296
N	24.706427	3.736613	-0.885542
C	26.001787	3.451681	-0.468086
C	27.411715	-2.125790	0.125213
N	26.376741	-3.059975	-0.005130
C	25.047943	-2.764682	-0.286515
O	26.822206	4.320644	-0.285536
O	22.648145	3.158377	-1.589735
O	28.545836	-2.519375	0.241189
O	24.208772	-3.627589	-0.400346
C	24.352582	5.128860	-1.153558
C	26.770378	-4.463968	0.093176
H	22.696639	-1.758073	-0.872019
H	27.457403	-4.717534	-0.714244
H	27.274822	-4.637720	1.043051
H	25.871118	-5.067816	0.025941
H	25.184142	5.751699	-0.839835
H	24.159921	5.268246	-2.217677
H	23.450352	5.389748	-0.601963
H	28.302698	2.462782	0.299808
C	29.326315	0.096751	0.858439
C	29.682654	-0.425192	2.065752
C	31.081219	-0.407220	2.288858
C	31.786425	0.129632	1.246874
S	30.718398	0.611699	-0.031416
C	33.225364	0.302910	1.113291
C	33.909567	1.321776	0.508287
C	35.320171	1.163046	0.575111
C	35.688320	0.028994	1.231066
S	34.323334	-0.875112	1.759509
H	28.960332	-0.805620	2.776678
H	31.552241	-0.756289	3.199348
H	33.417034	2.172292	0.052964
H	36.028638	1.870289	0.163325
H	36.686038	-0.333207	1.431022
C	21.622277	0.597416	-1.257949
C	20.949467	0.209451	-2.377929
C	19.560770	0.496072	-2.319177
C	19.183519	1.077177	-1.141473
S	20.544992	1.271307	-0.085165
C	17.853307	1.481888	-0.709163
C	17.487503	2.577747	0.020164
C	16.088556	2.650514	0.251617
C	15.405151	1.600169	-0.282426
S	16.470742	0.511941	-1.101826
C	13.941372	1.393420	-0.290521
C	13.275888	0.403639	0.419071
C	11.874861	0.251588	0.271132
C	11.131491	1.127216	-0.549290
C	11.825946	2.151542	-1.226780
C	13.186103	2.263979	-1.107652
C	11.186358	-0.787477	0.932648
C	9.841123	-0.952959	0.747472
C	9.083799	-0.089556	-0.079203
C	9.727880	0.975789	-0.695242
C	11.904162	-1.743726	1.815884
C	13.991197	-0.468800	1.400631
N	13.263915	-1.510487	1.986486
C	11.109349	3.113120	-2.103728
C	8.974820	2.031418	-1.442681
N	9.726678	2.977111	-2.150273
C	14.010003	-2.374882	2.898640
C	8.958912	3.950192	-2.924471
O	11.690668	3.971562	-2.725624
O	7.771474	2.112701	-1.451711
O	15.145854	-0.306981	1.709756
O	11.336659	-2.660079	2.363311
H	9.352232	-1.788050	1.235755
H	13.696048	3.039964	-1.666365
H	18.197290	3.323491	0.355800
H	15.605173	3.445860	0.805141
H	21.440058	-0.242174	-3.231227
H	18.866733	0.298230	-3.126624
H	9.660154	4.566736	-3.477597
H	8.290036	3.427854	-3.607250
H	8.357587	4.569597	-2.258535
H	14.873832	-2.793958	2.384164
H	14.362723	-1.798912	3.754417
H	13.343949	-3.165835	3.228283
C	7.660386	-0.424581	-0.265451
C	7.023879	-0.783062	-1.416198
C	5.664700	-1.125087	-1.216059
C	5.271779	-1.027132	0.090750
S	6.586290	-0.498584	1.089204
C	3.958664	-1.282028	0.663112
C	3.642654	-1.867011	1.857651
C	2.244529	-1.942990	2.084183
C	1.506487	-1.442180	1.051770
S	2.527703	-0.808441	-0.191855
H	7.518803	-0.803598	-2.378643
H	5.001041	-1.460865	-2.003078
H	4.388685	-2.253112	2.541030
H	1.796297	-2.383012	2.966457
C	0.038463	-1.297231	1.005367
C	-0.800340	-1.880284	0.064824
C	-2.185201	-1.579568	0.072317
C	-2.743632	-0.744499	1.064051
C	-1.878971	-0.210530	2.042868
C	-0.534581	-0.466605	1.995682
C	-3.043303	-2.098557	-0.920345
C	-4.368855	-1.761783	-0.933499
C	-4.942146	-0.916409	0.046752

C	-4.130769	-0.444144	1.071729
C	-2.394913	0.666794	3.125052
C	-4.687430	0.299881	2.244861
N	-3.771746	0.856736	3.146222
C	-0.297632	-2.896864	-0.907952
C	-2.527514	-2.992931	-1.989621
N	-1.181329	-3.329473	-1.902439
O	0.815004	-3.361585	-0.862046
O	-3.238643	-3.415457	-2.871298
O	-1.664927	1.168312	3.948024
O	-5.868261	0.425813	2.456105
C	-0.634943	-4.275384	-2.873148
C	-4.349440	1.628364	4.244781
H	0.108857	-0.004900	2.735258
H	-4.986981	-2.141114	-1.738924
H	-0.362399	-5.206550	-2.375735
H	-1.395234	-4.461476	-3.624803
H	0.258546	-3.853485	-3.331417
H	-3.534093	2.065547	4.811939
H	-4.996336	2.408050	3.844787
H	-4.947488	0.979085	4.884760
C	-6.359796	-0.560146	-0.136716
C	-6.905505	0.678330	-0.305230
C	-8.295418	0.644116	-0.568056
C	-8.806456	-0.625223	-0.598974
S	-7.564981	-1.793812	-0.289391
C	-10.177130	-1.050403	-0.833224
C	-10.624365	-2.155163	-1.506205
C	-12.035357	-2.260928	-1.527971
C	-12.659323	-1.240370	-0.873766
S	-11.508370	-0.132357	-0.208636
H	-6.323828	1.589322	-0.248918
H	-8.896087	1.525365	-0.756274
H	-9.958025	-2.856320	-1.993249
H	-12.574579	-3.062969	-2.015274
C	-14.105249	-0.972839	-0.775024
C	-14.569194	0.237240	-1.343331
C	-15.898442	0.556995	-1.389973
C	-16.865845	-0.337922	-0.886378
C	-16.418190	-1.544081	-0.305483
C	-15.033730	-1.844140	-0.218657
C	-17.388224	-2.448684	0.175956
C	-18.722283	-2.168203	0.048408
C	-19.183014	-0.966944	-0.536354
C	-18.248920	-0.037170	-0.971020
C	-18.657422	1.315742	-1.463127
C	-16.296022	1.846080	-2.013796
C	-16.992613	-3.735137	0.804728
C	-14.618019	-3.055677	0.555909
N	-17.656565	2.130430	-2.005851
N	-15.626315	-3.940544	0.956277
O	-13.475148	-3.292962	0.859755
O	-17.809131	-4.544572	1.178575
O	-15.484079	2.607260	-2.486083
O	-19.786996	1.733551	-1.401344
H	-13.858003	0.929120	-1.779643
H	-19.441419	-2.902079	0.393370
C	-15.177184	-5.141625	1.657376
C	-18.100246	3.420471	-2.530058
H	-14.664002	-4.865632	2.578451
H	-16.051216	-5.745183	1.879894
H	-14.482860	-5.697953	1.028351
H	-17.242244	3.911782	-2.977498
H	-18.880988	3.265229	-3.273673
H	-18.506699	4.032134	-1.724280
C	-20.643579	-0.813353	-0.688154
C	-21.372380	-0.854022	-1.838207
C	-22.768121	-0.751823	-1.614234
C	-23.093102	-0.636327	-0.291020
S	-21.666851	-0.643641	0.695380
C	-24.410923	-0.496178	0.309597
C	-24.878672	-1.014628	1.484879
C	-26.224178	-0.654295	1.754363
C	-26.779534	0.111478	0.772091
S	-25.630505	0.454566	-0.473866
H	-23.512667	-0.790082	-2.399553
H	-20.919507	-0.956816	-2.816147
H	-24.283745	-1.654910	2.124263
H	-26.774556	-0.977175	2.629441
C	-28.126043	0.717748	0.770165
C	-29.125956	0.438132	-0.152608
C	-30.346065	1.159661	-0.109432
C	-30.563174	2.127318	0.893230
C	-29.559541	2.359605	1.853842
C	-28.373673	1.679687	1.780698
H	-27.597987	1.895017	2.506153
C	-28.990460	-0.667237	-1.148540
C	-31.362124	0.944613	-1.067450
C	-32.533503	1.663848	-1.020001
C	-32.744335	2.621996	-0.015814
C	-31.773256	2.849343	0.929191
C	-31.182686	-0.059714	-2.147081
C	-29.763465	3.362367	2.935657
C	-32.000071	3.866942	1.989182
N	-30.980707	4.047287	2.925095
N	-29.999966	-0.792723	-2.109463
O	-28.070771	-1.448513	-1.150517
O	-32.019979	-0.240474	-3.000578
O	-28.922832	3.573409	3.777204
O	-33.016758	4.517126	2.055244
C	-29.804284	-1.846561	-3.102809
C	-31.226976	5.048899	3.960145
H	-33.666270	3.189469	0.027929
H	-33.287626	1.475695	-1.774841
H	-29.814435	-2.823594	-2.618965
H	-30.610012	-1.779205	-3.826614
H	-28.840230	-1.713217	-3.591866
H	-30.373972	5.056319	4.631039
H	-31.355639	6.030148	3.503012
H	-32.136530	4.799013	4.505649

E = -10643.7192087 Hartree

P(NDI2OD-T2), n = 5, UωB97X-D/6-31G*, charged state

C	25.813369	0.250643	-0.858830
C	24.910526	-0.673899	-1.425397
C	23.573454	-0.385442	-1.492894
C	23.046483	0.843902	-1.034299

C	23.921297	1.787464	-0.512934
C	25.301077	1.483036	-0.398421
C	26.199347	2.401780	0.185068
C	27.522295	2.081956	0.325765
C	28.048134	0.847339	-0.121543
C	27.195254	-0.051833	-0.747879
C	23.460771	3.160554	-0.142990
N	24.386870	4.006044	0.478310
C	25.731058	3.720604	0.686028
C	27.702969	-1.306091	-1.386853
N	26.750381	-2.211775	-1.868750
C	25.379505	-1.988649	-1.934836
O	26.477986	4.503247	1.226025
O	22.347104	3.567532	-0.365123
O	28.874721	-1.560868	-1.517426
O	24.618267	-2.808447	-2.392964
C	23.882971	5.318753	0.876717
C	27.279318	-3.451937	-2.432407
H	22.898762	-1.129846	-1.898920
H	27.855383	-3.238814	-3.333553
H	27.936073	-3.931419	-1.708046
H	26.439876	-4.097036	-2.671161
H	24.688871	5.849879	1.372810
H	23.549736	5.871756	-0.001450
H	23.036111	5.198596	1.551642
H	28.177335	2.793553	0.814841
C	29.472315	0.590618	0.164861
C	30.007226	-0.340057	1.003782
C	31.416012	-0.241114	1.118196
C	31.948871	0.767639	0.363735
S	30.703962	1.602752	-0.508070
C	33.342803	1.161276	0.219854
C	33.862298	2.417381	0.065598
C	35.278999	2.426277	-0.044738
C	35.817014	1.178618	0.029883
S	34.605946	-0.029485	0.214769
H	29.405866	-1.071691	1.528211
H	32.016912	-0.877601	1.755834
H	33.248798	3.310123	0.057225
H	35.869822	3.325526	-0.163013
H	36.858735	0.897105	-0.017340
C	21.582454	1.005768	-1.138289
C	20.844658	1.055474	-2.283376
C	19.450140	1.157774	-2.041872
C	19.135735	1.156239	-0.711632
S	20.565119	1.017114	0.260208
C	17.825259	1.240504	-0.084697
C	17.479973	1.853866	1.086563
C	16.094593	1.753963	1.379370
C	15.400672	1.050109	0.442195
S	16.439691	0.511003	-0.830761
C	13.937454	0.839277	0.390344
C	13.296066	-0.372592	0.605040
C	11.887583	-0.457315	0.475313
C	11.116437	0.685852	0.172703
C	11.789967	1.911361	-0.011149
C	13.155357	1.974386	0.083256
C	11.217329	-1.688691	0.640635
C	9.862110	-1.766359	0.472642
C	9.075707	-0.631769	0.156119
C	9.704423	0.602746	0.049853
C	11.965083	-2.930742	0.967431
C	14.051542	-1.588695	1.035326
N	13.337211	-2.785556	1.145606
C	11.044759	3.155788	-0.333852
C	8.931423	1.876733	-0.091967
N	9.660906	3.043500	-0.358594
C	14.119171	-3.961566	1.521274
C	8.870739	4.255080	-0.567585
O	11.608615	4.205114	-0.543309
O	7.734013	1.949991	0.026062
O	15.230171	-1.577812	1.294285
O	11.414470	-4.000606	1.082593
H	9.385248	-2.735280	0.565220
H	13.646120	2.924578	-0.091098
H	18.191028	2.389718	1.703037
H	15.627147	2.182280	2.257189
H	21.291938	1.055583	-3.269680
H	18.706466	1.254532	-2.823021
H	9.548280	5.047509	-0.868892
H	8.124031	4.075393	-1.339562
H	8.355903	4.531575	0.353133
H	14.915632	-4.120565	0.794769
H	14.570379	-3.811236	2.501975
H	13.449257	-4.815135	1.541363
C	7.642291	-0.859684	-0.089909
C	6.936287	-0.623204	-1.232216
C	5.584533	-1.034346	-1.147141
C	5.264046	-1.584087	0.064388
S	6.640107	-1.590619	1.118151
C	3.977859	-2.085527	0.523885
C	3.712951	-3.173642	1.307205
C	2.328423	-3.347755	1.565559
C	1.549111	-2.407712	0.960025
S	2.513902	-1.255623	0.105031
H	7.377118	-0.169904	-2.110940
H	4.871840	-0.952583	-1.958175
H	4.484415	-3.843726	1.666423
H	1.917376	-4.157169	2.155784
C	0.085233	-2.244941	1.091273
C	-0.841290	-2.449383	0.075938
C	-2.212419	-2.195810	0.311043
C	-2.674148	-1.773171	1.577403
C	-1.716832	-1.618888	2.601346
C	-0.384673	-1.834040	2.354041
C	-3.165685	-2.354285	-0.720484
C	-4.476910	-2.049968	-0.501663
C	-4.961793	-1.585438	0.752945
C	-4.052403	-1.505217	1.810379
C	-2.114819	-1.206844	3.970242
C	-4.483157	-1.256590	3.218742
N	-3.476524	-1.063192	4.180892
C	-0.428241	-2.999032	-1.249899
C	-2.761771	-2.813538	-2.073847
N	-1.410560	-3.111419	-2.236519
O	0.700133	-3.354325	-1.495802
O	-3.553123	-2.933777	-2.979442
O	-1.302296	-1.030251	4.850968
O	-5.632940	-1.233275	3.581971
C	-0.959075	-3.620406	-3.528769
C	-3.940950	-0.763529	5.533044
H	0.323807	-1.672331	3.157875
H	-5.163120	-2.135894	-1.335932
H	-0.541451	-4.620044	-3.408843

H	-1.813926	-3.645539	-4.196834
H	-0.183379	-2.968709	-3.930868
H	-3.071448	-0.534195	6.140876
H	-4.624564	0.083820	5.507307
H	-4.472862	-1.621261	5.946014
C	-6.362414	-1.170625	0.792783
C	-6.905277	-0.029999	1.320743
C	-8.275602	0.130449	1.036180
C	-8.801976	-0.897649	0.290766
S	-7.584077	-2.081164	-0.051984
C	-10.159216	-1.081381	-0.175330
C	-10.593641	-1.758498	-1.286974
C	-11.994022	-1.714078	-1.456701
C	-12.637577	-1.007347	-0.479842
S	-11.507011	-0.396646	0.677418
H	-6.324212	0.690516	1.880534
H	-8.860431	0.988243	1.343120
H	-9.918180	-2.248164	-1.979274
H	-12.524300	-2.192103	-2.269319
C	-14.070374	-0.674715	-0.368090
C	-14.412510	0.665268	-0.401154
C	-15.741505	1.092850	-0.422124
C	-16.793273	0.153293	-0.443268
C	-16.454751	-1.236793	-0.381152
C	-15.103139	-1.650269	-0.313037
C	-17.507994	-2.174260	-0.377973
C	-18.833593	-1.749964	-0.492431
C	-19.171862	-0.412035	-0.579223
C	-18.144108	0.566005	-0.511279
C	-18.449151	1.997389	-0.426520
C	-16.011074	2.525116	-0.455106
C	-17.241696	-3.604792	-0.285166
C	-14.812112	-3.069926	-0.097639
N	-17.361027	2.882292	-0.449634
N	-15.898581	-3.956509	-0.140941
O	-13.701992	-3.527755	0.122770
O	-18.117485	-4.457170	-0.312927
O	-15.133969	3.376577	-0.471525
O	-19.572569	2.464265	-0.328896
H	-13.641249	1.425327	-0.450795
H	-19.602241	-2.512320	-0.546762
C	-15.571795	-5.363426	0.036474
C	-17.698237	4.297159	-0.402552
H	-15.116671	-5.523332	1.015268
H	-16.494037	-5.929710	-0.050467
H	-14.854457	-5.678667	-0.722378
H	-16.773597	4.860668	-0.481322
H	-18.372604	4.546859	-1.222437
H	-18.207180	4.531920	0.534031
C	-20.591558	-0.087795	-0.823124
C	-21.159677	0.483731	-1.924980
C	-22.568840	0.564540	-1.852034
C	-23.082017	0.050501	-0.689788
S	-21.802688	-0.524452	0.332265
C	-24.471606	-0.053179	-0.290558
C	-25.071393	-0.987126	0.515149
C	-26.456145	-0.761109	0.690762
C	-26.924614	0.319653	-0.006544
S	-25.627669	1.118931	-0.833351
H	-23.193643	0.956038	-2.646625
H	-20.570764	0.838822	-2.760317
H	-24.534094	-1.823092	0.944448
H	-27.100556	-1.400921	1.282425
C	-28.291872	0.851079	0.031350
C	-29.055731	1.217901	-1.074004
C	-30.307289	1.862668	-0.888961
C	-30.822895	2.059352	0.408557
C	-30.075694	1.608354	1.516892
C	-28.846089	1.042364	1.326805
H	-28.263855	0.753358	2.193970
C	-28.671266	0.841286	-2.465230
C	-31.062434	2.333610	-1.986151
C	-32.270724	2.963542	-1.790141
C	-32.782876	3.140777	-0.497671
C	-32.067223	2.692783	0.588402
C	-30.563586	2.166170	-3.375065
C	-30.598235	1.779326	2.898871
C	-32.613483	2.881684	1.956721
N	-31.840068	2.413153	3.018727
N	-29.389960	1.438090	-3.513652
O	-27.802413	0.047392	-2.726698
O	-31.157617	2.616597	-4.329645
O	-29.990664	1.394073	3.869659
O	-33.680375	3.413933	2.163351
C	-28.917314	1.132912	-4.861664
C	-32.395783	2.610930	4.354383
H	-33.736647	3.628492	-0.335989
H	-32.813596	3.318813	-2.657848
H	-29.076673	0.077541	-5.086859
H	-29.473866	1.750774	-5.559154
H	-27.850951	1.342267	-4.929704
H	-31.685455	2.220187	5.075904
H	-32.566732	3.673090	4.529119
H	-33.348847	2.088795	4.441849

E = -10643.8136191 Hartree